6

Io's Atmosphere and Neutral Clouds

Nicholas M. Schneider
University of Arizona, Tucson

William H. Smyth
AER, Incorporated, Cambridge

Melissa A. McGrath
University of Virginia, Charlottesville

Abstract

Much of our basic understanding of the Io atmosphere, neutral clouds, and plasma torus has come from the study of variations in their morphology, density, and energy distribution. This chapter discusses the time variabilities inherent in the physical processes that govern the behavior of the system, and their relative importance in proposed models of the Io atmosphere. Observations are discussed and compared to model predictions, and new constraints are placed on these models. The variations are then examined in the context of the complete neutral-cloud/plasma torus system, and the unsolved problem of overall system stability is discussed. Several possible mechanisms responsible for the stability are described and evaluated. Future observations of time-variable phenomena show great promise for probing the nature of the atmosphere and its complex interaction with the plasma torus.

OVERVIEW OF THE SYSTEM

This review emphasizes time variabilities of the neutral species in Io's vicinity at the expense of a discussion of our best understanding of the underlying steady-state behavior. The major issues concerning the "average" state of the atmosphere and extended neutral clouds are well reviewed in Brown et al. (1983), Kumar and Hunten (1982), Nash et al. (1986), and Johnson and Matson (1989). Time-variable phenomena have proven to be powerful tools for determining the nature of the atmosphere and neutral clouds, but considerable potential remains untapped.

Nomenclature and Definitions

Figure 34 defines the terminology used in this chapter. The term *lower atmosphere* will refer to atoms and molecules gravitationally bound to Io and confined to an altitude less than or comparable to an Io radius (R_{Io} = 1815 km). It is generally agreed that the dominant atmospheric constituent near the surface is SO_2, but the value of the surface pressure is currently under heated debate (cf., Johnson and Matson, 1989, for a summary). If the column abundance exceeds $\sim(3 \times 10^{14})$ molecules per square centimeter, the atmosphere is considered collisionally thick. The altitude of the transition between the collisionally thick and thin regimes is called the exobase, and the collisionless region, called the corona or exosphere, extends out to $\sim 10^4$ km. Jupiter's gravity dominates outside this radius; atoms and molecules beyond this distance are not considered part of the atmosphere but are considered part of the neutral clouds.

The neutral clouds are huge in comparison, extending out hundreds of thousands of kilometers into the toroidal volume surrounding Io's orbit. To date four neutral gas clouds, as summarized in table 5, have been detected by remote observations of cloud emission lines. A fifth cloud of SO_2 (or S_2) has been proposed as a result of the in situ detection of SO_2^+ (or S_2^+) in the plasma torus. Sodium and potassium are present only in trace amounts but are most readily visible (see table 5). Atoms and molecules in the neutral clouds would form complete gas tori around Jupiter were it not for their finite lifetimes in the plasma torus, which limit their morphologies to partial tori of varying angular extent. The sodium cloud with a short lifetime against electron impact ionization fills only a small portion of the orbital circumference (fig. 34). This short lifetime makes sodium quite responsive to changes in plasma conditions, and the study of changes in the sodium cloud has been instrumental in our remote sensing of the jovian magnetosphere.

Despite their different spatial scales, the neutral clouds are intimately linked to the Io atmosphere through the corotating plasma torus. (See Strobel and Bagenal, this volume, for further discussion of the plasma torus.) The neutral clouds are simultaneously created and destroyed by the torus through a variety of spatially and temporally varying processes. The careful examination of time variabilities is an underutilized tool for probing the interconnection of the surface, atmosphere, corona, clouds, and plasma.

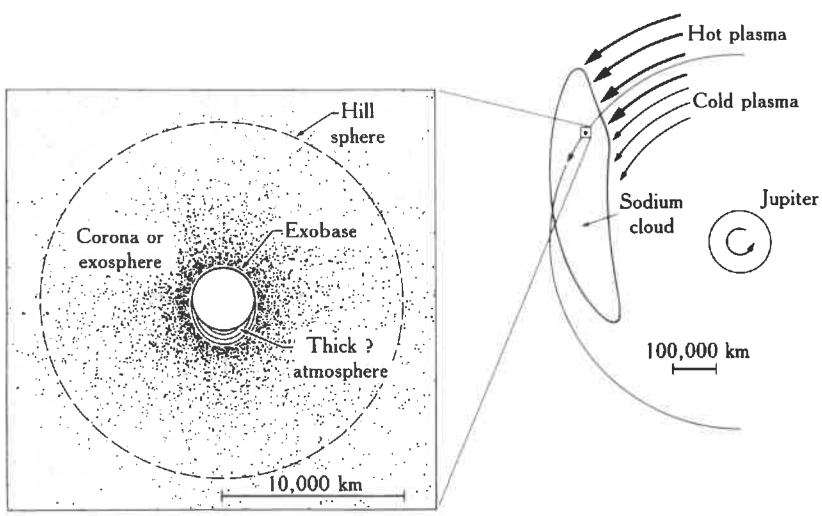

Figure 34. Simplified view of the atmosphere and sodium cloud. The left half illustrates Io's immediate vicinity. The contours schematically show the thick atmosphere, concentrated in this example on the sunlit hemisphere. The thin corona (or exosphere) is represented by the *dots*. The *dashed line* shows the location of the Hill sphere, the effective limit of Io's gravity. The scale of the right half of the figure is reduced by a factor of 40 to show the neutral sodium cloud outline (adapted from Smyth and McElroy, 1978). The corotating plasma, indicated by the *arrows*, travels at 75 km/s, overtaking the neutrals that orbit Jupiter at 17 km/s. The cloud lies preferentially inside Io's orbit because the plasma is cooler there and less able to ionize the sodium. Inside Io's orbit, the cloud extends forward, but not backward, because sodium atoms closer to Jupiter travel faster than Io.

Table 5. Io's Neutral Gas Clouds

	First detection		Cloud emission		
Neutral cloud	**Date**	**Observer**	**Wavelength (Å)**	**Intensity (Rayleighs)**	**Excitation mechanisms**
Sodium	1972	Brown (1974)	5890, 5896	10^3–10^4	Resonance scattering
Potassium	1975	Trafton (1975) Trauger et al. (1976)	7665, 7699	15–300	Resonance scattering
Oxygen	1980	Brown (1981)	6300	~8	Electron impact
Sulfur	1981	Durrance et al. (1983)	1304, 1425	~3	Electron impact

Important Neutral Sources and Sinks

We first discuss the processes responsible for creating and destroying the atmosphere and clouds, and determine their characteristic time scales and amplitudes of variability. Figure 35 shows the important processes schematically. Volcanoes are the initial source of the atmosphere, depositing ejecta on the surface and venting gas directly into the atmosphere. The SO_2 frost sublimates, also supplying the atmosphere. If the atmosphere is collisionally thin, plasma ions may impact the surface and liberate some of the surface atoms and molecules through sputtering. If the atmosphere is collisionally thick, corotating the plasma ions will interact with the gas through a collisional cascade process, transferring some of the energy and momentum of the ions to the neutrals. A fraction of the energized neutrals will escape directly into the distant neutral clouds, and the remainder will create a corona. The neutrals in the collisionally thin regions will be subjected to electron impact ionization, elastic collisions, and charge exchange. All the processes listed are time variable, each with a different amplitude and time scale. Table 6 summarizes the variabilities, and the processes are discussed individually below.

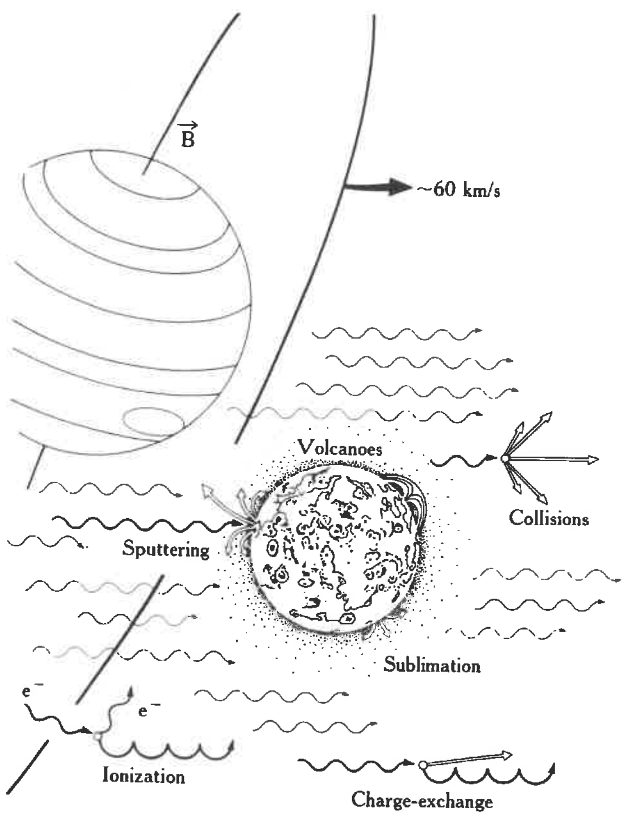

Figure 35. Sources and losses of neutrals at Io. Io is shown embedded in the flow of the corotating plasma. Ions, carried by magnetic field lines, are represented by *wiggly arrows*. Neutrals are shown as *outlined arrows*. The individual processes are discussed in the text.

Plasma Related Processes Ionization, elastic collision, charge exchange, and sputtering rates will all vary systematically with the flux of incident plasma. The plasma density and temperature in the torus is spatially nonuniform, so the flux will depend on Io's position in the magnetosphere. The plasma is confined within $\sim \pm 1\, R_J$ ($1\, R_J = 71{,}400$ km) of the centrifugal equator, which is tilted 7° with respect to Io's roughly circular orbit. The plasma corotates with Jupiter, making one revolution every ~10 hours. Io orbits Jupiter in ~42.5 hours, which thereby creates a ~13 hour period of the

Table 6. Variability of Important Processes

Process	**Variation amplitude**	**Time scale**
Ionization	2–20	6.5–42 hr
Sputtering	2	6.5–42 hr
Collisions and charge exchange	2–20	6.5–42 hr
Sublimation	large	42 hr
Volcanoes	large	days–years

plasma with respect to Io. The tilt of the plasma plane is the primary cause of systematic variations: Io appears to oscillate in magnetic latitude by $\pm 0.7\, R_J$, with a period of about 13 hours. In addition to these oscillatory effects, more complex but smaller motions of the plasma torus relative to Io's orbit are produced by the offset of the magnetic dipole from the center of Jupiter and the presence of an east-west electric field in the planetary magnetosphere.

The rates for ionization, elastic collisions, and charge exchange are straightforward to calculate in the low-density regions far from Io. The plasma properties will be essentially unchanged by interactions with the atoms and molecules, and plasma-related reaction rates for these neutral gases will vary linearly and instantaneously with the time-varying incident plasma flux. Near Io, however, the incident flux and its effects on the corona and atmosphere may be substantially altered, both by the presence of Io's solid body (Wolf-Gladrow et al., 1987; Barnett, 1986) and by interaction with gas in the extended atmosphere (e.g., Sittler and Strobel, 1987). Although evidence of both types of plasma alteration have been observed, it is difficult to estimate the magnitude of these effects near Io. For the moment we can only say that the situation very near Io is significantly more complicated than elsewhere in the neutral clouds.

We consider first the case of electron impact ionization in the neutral clouds. In this reaction, a torus electron ionizes an atom and thereby removes it from the neutral cloud. The fresh ion is accelerated to corotation velocity with a large gyration velocity, adding mass and energy to the plasma. The lifetime against electron impact ionization depends on the electron density and temperature, and will be shortest when Io passes through the centrifugal equator. Taking the case of sodium, figure 36 shows how the spatial structure of the ionization rate maps into a temporal variation. For sodium near Io's position, the lifetime against ionization varies from ~1.3 hours on the plasma equator to ~4 hours when farthest from the equator. Note that the minimum lifetime occurs twice during a full cycle (ignoring magnetic longitude varations), so the effective period is 6.5 hours if magnetic longitude variations are unimportant. For sodium on trajectories far north or south of Io, the amplitude of variation is much larger. Only one minimum lifetime occurs each cycle, so the period there is 13 hours. Atoms on such out-of-plane orbits move through regions of different ionization lifetime, so more detailed calculations are required to determine the magnitude of the variation.

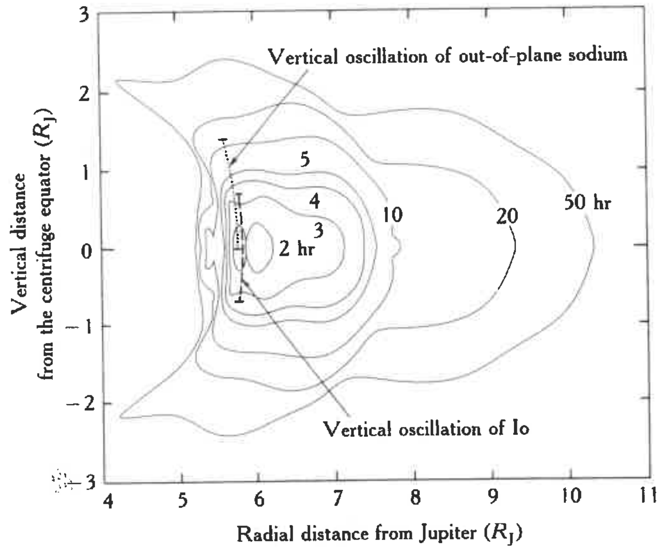

Figure 36. Spatial variation of sodium lifetime against electron impact ionization. Contour labels indicate the lifetime in hours. The rapid rise in lifetime inside about 5.7 R_J is due to a sudden drop in electron temperature. Io's motion, using the tilted dipole approximation to Jupiter's magnetic field, is indicated by the *dashed line*. The *dotted line* shows the range of lifetimes experienced by sodium already out of Io's orbital plane. When the offset of the tilted dipole is included, the lines open up into slightly tilted ovals. When the east-west electric field is incorporated, the contour values also change as a function of orbital longitude. Adapted from Smyth and Combi (1988a).

Io's motion through the plasma is actually more complicated than indicated by the tilted dipole approximation, further modulating the density and temperature of the plasma impacting Io. The axis of the dipole is offset by ~0.13 R_J from Jupiter's rotation axis, so in the magnetic coordinate system Io appears to move inward and outward in addition to its north-south motion. Furthermore, there appears to be an electric field across the entire jovian magnetosphere fixed in Sun-centered coordinates (Barbosa and Kivelson, 1983; Ip and Goertz, 1983; Goertz and Ip, 1984). This field effectively pulls the plasma torus at Io's orbit ~0.15 R_J further away from Jupiter on the east (as seen from the Earth), and toward Jupiter on the west. As a result, the plasma at Io's orbit is on average denser and hotter in the west than in the east. Smyth and Combi (1988a) have constructed a detailed model of the sodium cloud that incorporates these epicyclic offsets. All of these effects operate simultaneously, so variabilities with periods of 6.5, 13, and 42 hours are superposed in the rates of plasma-related processes.

Table 7. Atomic Lifetimes for Plasma-Related Reactions[a]

Atom	Electron impact ionization (hours)	Charge exchange[b] (hours)	Elastic collision[c] (hours)
Sodium	1.3	22	16
Potassium	1.1	11	24
Oxygen	55	18	13
Sulfur	10	13	21

[a] All rates calculated in the centrifugal equator at Io's radial distance. [b] Based on cross sections from Johnson and Strobel (1982). [c] Based on Thomas-Fermi momentum-transfer cross sections with minimum velocity transfer of 2 km/s. The cross section increases for smaller minimum transfers, but a better knowledge of the interaction potential between these ions and atoms is required before more detailed calculations are warranted.

Next we consider elastic collisions and charge-exchange reactions, whose rates depend primarily on the plasma density. In elastic collisions, the incident ions impact the slow neutrals in collisions similar to billiard-ball-type knock-on collisions. Glancing blows are most likely, sending the neutrals off nearly perpendicular to the plasma flow at low velocities. In the less probable head-on collisions, the neutrals are ejected more in the forward direction and at much higher velocities. In charge-exchange reactions, a corotating ion strips an electron from a neutral during a glancing collision, thus becoming a very fast neutral. Forward-directed escaping atoms are the most likely product. Because of the motion of the plasma torus relative to the satellite orbital plane, rates for elastic collisions and charge exchange should show time variations comparable to those of electron impact ionization. The primary difference lies in the fact that ionization acts as a sink of slow neutrals in the clouds, whereas elastic collisions and charge-exchange reactions act primarily as sources of fast neutrals. The relative importance of these processes and electron impact ionizations (based on undisturbed plasma properties at Io's orbit) for each neutral constituent are summarized in table 7. The lifetime of neutrals for these reactions is different for each species. For sodium and potassium, electron impact ionization dominates charge exchange and elastic collisions by order of magnitude, whereas for sulfur and oxygen the three processes have more comparable values. These calculations apply only to plasma properties on the centrifugal equator at Io's distance; the lifetimes vary significantly both radially and normal to the equator.

Sputtering occurs from a collisionally thick target, either Io's surface or the atmospheric exobase. In the simplest analysis, the rate of sputter removal from the target is SR = *incident ion flux* × *yield per ion* × *effective area sputtered.* Relative sputtering rates for various conditions on Io are summarized in table 8 and explained below. The single biggest factor controlling the sputter removal rate is the presence or absence of a thick atmosphere on Io. The rate varies roughly as the cube of the exobase radius: two powers for the geometrical increase in the projected size, and one power for the lower gravitational binding energy. Surface sputtering is considerably less efficient since the molecules are more tightly bound in a solid; the tabulated value assumes the entire surface is covered by SO_2, the most easily sputtered Io surface component. For some constituents, especially SO_2, the sputtering rate is a very strong function of temperature (Lanzerotti et al., 1982). The sputtering rate, like the elastic collision rate, depends linearly on the ion density.

The surface sputtering yield also depends on the mass and energy of the incident ions, and the composition of the surface. More massive and energetic ions produce a higher yield, but the flux of such ions on Io may be too low to contribute appreciably to the sputtering rate (Lanzerotti et al., 1982). SO_2 frost is sputtered more efficiently than sulfur, and smooth surfaces allow easier escape than do porous surfaces. Sputtering from

Table 8. Relative SO_2 Supply Rates for Various Atmospheric and Surface Conditions[a]

Exobase at 1800 km altitude[b] (radius = 2 R_{Io})	8.0
Exobase at 900 km altitude[b] (radius = 1.5 R_{Io})	3.4
Exobase at 0 km altitude (radius = 1 R_{Io})	1
Dayside surface only[c] (110 K)	0.22
Nightside surface only[c] (90 K)	0.11

[a] From McGrath and Johnson (1987) and Lanzerotti et al. (1982). [b] Spherically symmetric atmosphere. [c] Maximum possible rate, using 100 percent SO_2 surface coverage and ignoring surface porosity effects.

warmer, dayside surfaces is more efficient than from the nightside; the yield from Io's hot spots is also probably quite high but has not been estimated quantitatively.

Atmospheric sputtering may differ significantly from surface sputtering in a qualitative sense. The atmosphere absorbs an immense momentum flux from the plasma, and only a small fraction goes to the atoms directly sputtered out. The remainder of the input, called ion heating, may be responsible for further ejection from the atmosphere, which may dominate the escape. This process is not well understood, and it may not be subject to the same variations assigned to standard sputtering in the subsequent paragraph. Furthermore, thick atmospheres (and their concomitant ionospheres) are likely to generate a substantial deflection of the plasma flow. This too will strongly modify the atmospheric sputtering process, and the following discussion may not be appropriate. Progress on these issues is relatively recent, and a full analysis of their effects on time variability is premature.

Variabilities in the sputtering rate will be caused primarily by changes in the incident flux, the exobase level, and the temperature of the target. The incident flux for sputtering is subject to exactly the same variations as the collision and charge-exchange rate, and therefore should give rise to variations with periods from 6.5 to 42 hours. Diurnal cycles may affect both the surface temperature and the exobase level, leading to significant variability at the 42-hour orbital period.

One caution should be stressed pertaining to sodium: its physical and chemical state on the surface and in the atmosphere is completely unknown. Unlike SO_2, quantitative measures of its supply rate (akin to table 8) are unavailable, and it is not even clear whether an increase in the exobase level will enhance or decrease the sodium supply rate. If sodium is released only by surface sputtering, a high exobase will diminish the sputtered sodium; if sodium is always present in the atmosphere at a fixed mixing ratio, a high exobase level will lead to an increase in sodium supply. In either case, the sodium supply will still vary with changing atmospheric conditions. We make the assumption that nature does not conspire to equilibrate the release of a trace constituent, and that therefore variations in sodium supply will correlate with those in SO_2, even though a sign of the correlation is unknown. The supply of sodium from the surface is also problematic in its magnitude; current best estimates of the surface sputtering rate for sodium (Chrisey et al., 1987; Sieveka and Johnson, 1984) are well below the levels required to populate the cloud. The problem is alleviated if sodium is always present in a thick atmosphere at about the 1 percent level, but the issue of how sodium is injected into the atmosphere must be addressed.

Sputtering, elastic collisions, and charge exchange eject sodium from Io's vicinity over a large, nonthermal range of velocities. The speed determines the relative importance of the variations in the supply and loss rates. For sodium, slower atoms are most strongly affected by the variable sink. These atoms, generated by sputtering and multiple collision processes, travel at ~3 km/s, and are responsible for filling the region near Io and the forward cloud. The medium-speed sodium (3–30 km/s, the product of one or more elastic collisions) is less sensitive to the variable ionization rate since it travels more quickly out of the plasma, and is more sensitive to the changeable source rate. The highest speed sodium (30–100 km/s, created through charge exchange) is completely unaffected by the changing ionization rate, but responds directly to the variable source rate.

Surface Processes The source of the atmosphere, clouds, and torus is ultimately the extensive volcanic activity on Io. As discussed by McEwen et al. (this volume), the handful of smaller SO_2-driven plumes appear to be long-lived (~years) and fairly constant in number and size. In contrast, only one of the very large plumes is apparently active at any given time, with the eruption lasting only days to months and varying in size during its lifetime. These large plumes may be driven by sulfur vapor instead of SO_2 (McEwen and Soderblom, 1983), so the total volcanic output may change radically in composition as well as amount on this short time scale. The atmosphere, clouds, and torus will subsequently respond according to the strength of their link with the volcanoes.

The small volcanoes also emplace large surface deposits of SO_2 frost that may later sublimate. The equilibrium vapor pressure above these frosts is strongly temperature-dependent, varying by five orders of magnitude over a 40 K change in temperature between the subsolar and antisolar points. As discussed in the next section, this simplified case leads to an atmosphere that is much denser on the dayside than the nightside. As a result, the atmospheric sputtering rates should be higher when the corotating plasma impinges on the sunlit hemisphere, and lower on the dark side, leading to an oscillation in the supply to the neutral clouds during Io's 42-hour orbit around Jupiter.

Despite the compositional difference between the eruptions, the global surface composition has apparently remained fairly constant, as indicated by ground-based photometric data (reviewed by McEwen et al., this volume). The large volcanoes are apparently restricted to a specific longitude range; when they erupt, to first order they overlay the terrain with fresh deposits of the same composition. Therefore, the sublimation and surface sputtering processes, both of which depend on surface composition, would be expected to be relatively insensitive to changes in volcanic activity.

Characteristic Lifetimes of Components of the System

The time scales summarized in table 7 must be placed in the context of the replenishment times of potentially observable features. The replenishment times in table 9 are the ratio of estimated inventory of the regions of interest to the neutral supply rate. The rate used, $\sim(1.8 \times 10^{28})$ atoms per second (Smyth and Combi, 1986), is derived by extending the fairly well constrained loss rates from the sodium cloud to models of the oxygen and sulfur clouds.

A change in the region in question will be observable if the replenishment time is comparable to or less than the variation time scale. As table 9 indicates, the replenishment time of the lower atmosphere is too uncertain to determine the likelihood of observable variations. The large range of possible atmospheric lifetimes comes from our ignorance of the atmospheric thickness; an atmosphere with a subsolar pressure of 10^{-7} bar could supply the torus for half a year, ignoring other losses or changes. On the other hand, a thin atmosphere (i.e., a corona) must be regenerated on a time scale of hours. The sodium cloud, extending forward and inside Io's orbit, is composed of survivors of the harsh ionizing plasma near Io. Orbit calculations by Smyth and McElroy (1978) indicate that spatial extent of the observed cloud is consistent with a 20-hour formation time. Finally, the population of the plasma torus is considerably larger than the neutral population, so the lifetime is correspondingly longer. The value for SO_2 frost is included to show that the sputtering process cannot deplete the surface frost on a short time scale; the corona, neutral clouds, and plasma could be supplied for centuries by minimal surface frost.

Table 9. Replenishment Time Scales

SO_2 frost (1 mm)	400 years[a]
Thick atmosphere	2 hours–180 days[b]
Corona	1–2 hours
Extended cloud	~20 hours
Plasma torus	~60 days

[a] Assuming a density of 0.2 g/cm³ and 100 percent surface coverage.
[b] Assuming a pressure of 10^{-8} bar over the entire dayside hemisphere.

These simplistic calculations show that most of the predicted variations should be visible throughout the sodium cloud and down to the corona. Direct observations of the lower atmosphere would clearly be revealing, but no means of measuring its content on a sufficiently short time scale is currently possible. The long-time constant of the plasma torus suggests that it would respond only to the long-term effects of changing volcanism.

ATMOSPHERIC MODELS

We now examine the three major atmospheric models proposed to date, and determine the dominant time variabilities expected of them. Readers not familiar with these models are urged to consult Johnson et al. (1988). Predictions of the sodium cloud behavior are stressed below, since sodium is the most readily observed neutral constituent. For each atmospheric model, we assume that the neutral clouds and corona are generated by sputtering of the surface or, in the case of a thick atmosphere, sputtering and multiple collisions at the atmospheric exobase. We further assume that sulfur and oxygen ions in the corotating plasma are responsible for sputtering, and that there is no deflection of the plasma flow around Io. Variations on these assumptions are explored in section titled Feedback Loops between Neutrals and Ions.

Sputtered-Corona Model

In the absence of sublimation or volcanic activity, an extended but collisionally thin atmosphere will arise on Io simply from the impact of plasma torus ions on the surface (Watson, 1981). Sieveka and Johnson (1985, 1986) have computed model corona based on the impact of ions into an SO_2 surface. The model assumes a constant flux of ions impacting the trailing hemisphere surface, and does not include loss processes such as ionization. Only about 3 percent of the sputtered molecules directly escape from Io's gravity. Most of the molecules therefore travel on ballistic trajectories around Io, forming a neutral corona. The calculated corona of Sieveka and Johnson (1985) is shown in figure 37. The

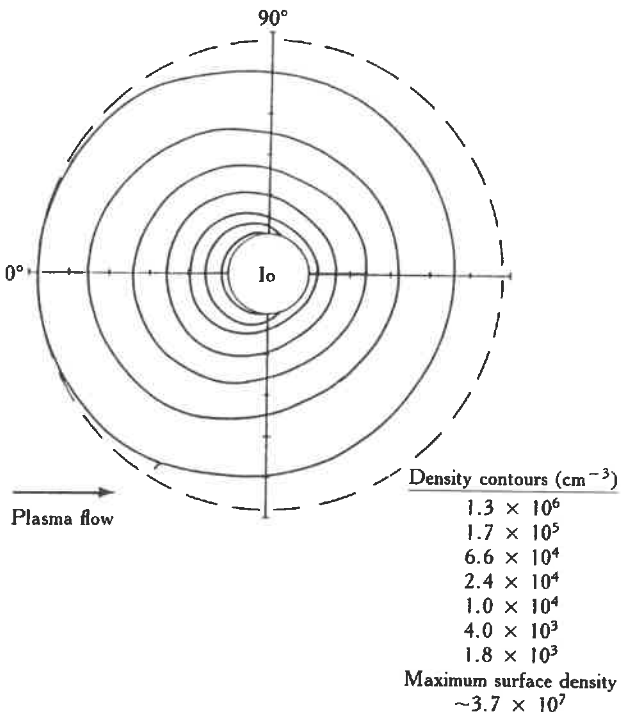

Figure 37. Theoretical model of a sputtered SO_2 corona. From Sieveka and Johnson (1985). The corona is densest above Io's trailing hemisphere.

density is highest over the trailing hemisphere where the incident flux is largest. The column abundance there is ~(4.5×10^{14}) molecules per square centimeter, about unit collisional thickness. The abundance over the leading hemisphere is lower by about an order of magnitude.

The effects of both a time-varying ion flux and neutral lifetime can, however, significantly alter this picture of the corona. The critical parameter that determines the density distribution in the corona is the ratio of the ballistic flight time to the atom-molecular lifetime. The density of atoms and molecules that have relatively long lifetimes in the plasma will be affected primarily by the changing flux of ions to the surface; high ion densities will lead to increased supply of these species. Short-lived species in the corona will not vary as much, since the increased sputtering rate will be approximately offset by the decreased lifetime. In either case, the variations will be fairly small, of the order of the factor of two variations in the plasma density. The strongest variation in the supply rate should have a period of 6.5 hours, but the offset dipole and east/west electric field will generate 13-hour and 42-hour modulations as well.

The temperature difference between the day and night sides will lead to another 42-hour period in SO_2 supply. Sputter yields from dayside SO_2 frosts at 110 K should be about twice the yield from the nightside 90 K frosts (Lanzerotti et al., 1982). Sodium compounds do not exhibit such a larger variation in sputtering rates with temperature, so the supply rate to the sodium clouds will not undergo this diurnal variation. In the absence of a thick atmosphere, changes in volcanic activity do not strongly affect the sputtering rates, so the sputtered-corona model would predict fairly constant densities in the atmosphere, clouds, and torus over the years.

Sublimated Atmosphere

There is considerable (albeit controversial) evidence for a thick SO_2 atmosphere maintained by sublimation, including the detection of gaseous SO_2 over a hot spot (Pearl et al., 1979), identification of SO_2 frost on the surface (Fanale et al., 1979; Hapke, 1979; Smythe et al., 1979), and the presence of a dense ionosphere (Kliore et al., 1975). A number of models have been developed to describe an SO_2 atmosphere in vapor pressure equilibrium with the surface, as reviewed in Johnson et al. (1988). Given the vapor pressure variation of five orders of magnitude over the range of possible Io temperatures, it is clearly essential to identify correctly the region of the surface controlling the equilibrium. Preliminary models (e.g., Pearle et al., 1979) used crude estimates of the average dayside temperatures; more recent studies (Fanale et al., 1982, "regional coldtrapping") have suggested that high-albedo SO_2 patches, much colder than the average surface temperature, dictate a lower atmospheric pressure. In regions lacking SO_2 frosts, coldtrapping in the insulated subsurface layers (Matson and Nash, 1983) may drive the atmospheric pressure lower still. McEwen et al. (1987), using the regional coldtrapping model, suggest that the maximum subsolar pressure is 10^{-8} bar (collisionally thick), with negligible pressure on the night side. This type of atmosphere is illustrated in figure 38.

Earth-based observations can clearly never view Io's night side, but a strong day-night atmospheric asymmetry should produce variations in the sputter-generated neutral clouds (figure 38). When Io is west of Jupiter, the plasma flow impacts the thick dayside atmosphere. Half an orbit (21 hours) later, the plasma strikes the nightside surface. Rough calculations for SO_2 show that the atmospheric sputter removal rate should be a factor of eight higher than the nightside

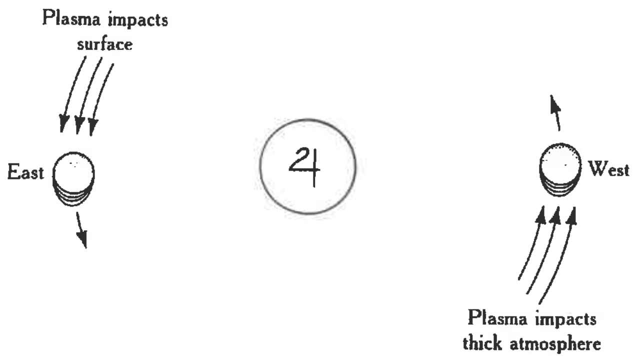

Figure 38. Supply asymmetry of the sublimated atmosphere model. The atmosphere is densest over the warm subsolar point. Ignoring other possible effects, the atmosphere's diurnal asymmetry leads to an orbital asymmetry in the sputtering rate. When Io is west of Jupiter, the plasma impacts the dayside atmosphere. 180° later, the plasma strikes the nightside surface.

surface sputtering rate, not allowing for less than 100 percent SO_2 surface coverage or a high dayside exobase. The formation rate of the neutral clouds of SO_2 and its byproducts should be much greater when Io is west of Jupiter. The level of sodium cloud asymmetry is more difficult to calculate, since we know neither the form sodium takes on the surface nor the process that releases it into the atmosphere. (See the section titled Overview of the System.) Nonetheless, it is unlikely that the supply rate to the sodium cloud could remain constant in the face of large changes in the SO_2 supply rate. In the sublimated atmosphere model, then, the 42-hour diurnal cycle and the plasma-induced variations discussed above should be observable.

Io may have a thick dayside atmosphere and no appreciable nightside atmosphere. This is unique in the solar system. Mechanisms have been proposed for an atmosphere on the dark hemisphere (see Johnson et al., 1988), but all share the feature that the nightside atmosphere is very different from the dayside atmosphere in composition and/or density. If there is a collisionally thick nightside atmosphere, the supply rate asymmetry may be greatly reduced, but probably not eliminated.

Volcano-Generated Atmosphere

Volcanoes have been suggested as the direct atmospheric source since the Voyager IRIS experiment detected gaseous SO_2 near an eruption. Only recently has this possibility been quantitatively explored (Moreno et al., 1987, Baumgardner et al., 1987). Their work concludes that even a single volcanic eruption can create a substantial atmosphere. A large Pele-type eruption (typically found in Io's inner trailing quadrant) would form a thick local atmosphere, with an exobase bulging to 500 km over the plume, where the surface pressure nears 10^{-6} bar (figure 39). The exobase level decreases away from the vent, intersecting the surface almost halfway around the planet. Almost all of the erupted gas rapidly condenses onto the cold surface, but the remaining few percent is evidently sufficient to create a thick atmosphere over much of the entire body. In the case of a smaller, Prometheus-type eruption, the exobase reaches only 200 km altitude, and drops to the surface 40° away from the vent.

Supply to the clouds and torus will therefore fall into two regions, dependent on the activity or dormancy of large eruptions. The largest, most variable plumes are favorably situated on Io for sputtering by corotating ions, so the supply rate will be directly linked to the presence or absence of such eruptions. Baumgardner et al. (1987) show that Pele-type eruptions lead to high escape rates characterized by atmospheric sputtering, whereas eruptions lead to a much lower rate characterized by surface sputtering. As table 8 shows, the numerical difference will be at least a factor of four. Baumgardner et al. suggest a factor of 20, including the effects of the high exobase and a more reasonable estimate of the fractional SO_2 surface coverage. Since the large eruptions tend to be short-lived and sporadic, the supply rate may change drastically on a time scale of days to weeks. Furthermore, if the Pele-type eruptions are compositionally different from

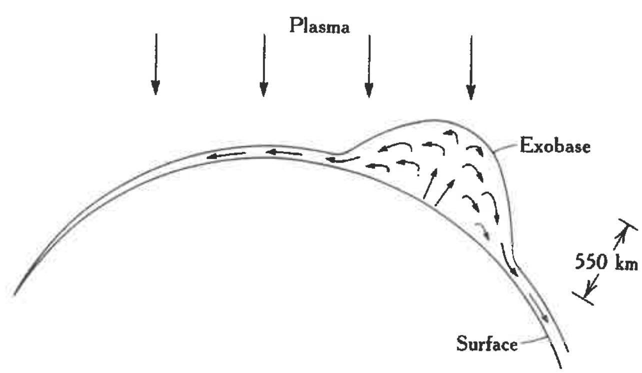

Figure 39. Simulation of a volcano-generated atmosphere for Io. The atmosphere is densest over the largest volcanic eruption, probably in Io's inner, trailing quadrant. The *solid line* schematically shows the exobase altitude. When no large eruptions are active, the atmosphere will be collisionally thin over most of the surface. Adapted from Baumgardner et al. (1987).

the effective surface composition, the clouds and torus may change composition rapidly.

Summary of Predicted Variations

Table 10 summarizes the predicted variabilities of the atmosphere and sodium cloud for each of the models outlined above. The sputtered corona is a fairly stable atmosphere; variations in density above a factor of two would not be expected. The variations should be roughly periodic, with periods ranging from 6.5 to 42 hours, but overlapping variations will distort the regular pattern. The SO_2 supply rate will be higher when the plasma impacts the warm, dayside surface than when it strikes the nightside surface, but the sodium supply rate will probably not vary with surface temperature. A detailed model is necessary to predict the phase lag of the brightness oscillation behind the oscillating supply and loss rates. No large secular changes would be expected.

The dominant variation in the sublimated atmosphere model is caused by the atmosphere's day-night asymmetry. The dayside atmospheric sputtering rate should be a factor of eight higher than the nightside surface value. Some form of orbital asymmetry in the sodium cloud should result, although its exact form is not clear. The presence of a nightside atmosphere will tend to reduce the supply rate variation. Short-term plasma-induced variations will also be present, but at a lower level than the diurnal effect. Again, there are no obvious causes of large secular changes.

The volcano-generated atmosphere would be the most variable on a time scale of days to months. The neutral supply rate may vary by over an order of magnitude, with corresponding changes in composition. These variations would not be periodic, but linked to the erratic eruptions of the large plumes. The compositional change is harder to address quantitatively, but may be quite significant in terms of supply to the plasma torus.

It is, of course, overly simplistic to discuss the models exclusively. Almost certainly, all atmospheric sources are active at some level: Volcanoes create at least a local atmosphere, and the sputtered corona will form above a thick atmosphere regardless of its source. But one of the atmospheric sources, that is, sputtering, sublimation, or volcanic venting, will dominate, and its variability (listed in table 10) will be appropriate.

Table 10. Atmospheric Models: Supply Variations

Model	Variation amplitude	Time scale
Sputtered corona	2	6.5–42 hours
SO_2 sublimation	4	42 hours
Volcanic outgassing	4–20	days–years

In the discussion that follows, we compare these predictions with the observed variations, with the goal of determining which model is most consistent with the data, and what additional constraints can be placed on the models if they are to reproduce the observed behavior.

OBSERVED VARIATIONS

Ideally, one would choose to compare the above predictions against the observed overall state of the atmosphere and neutral clouds. Unfortunately, the dominant constituents, namely SO_2, S, and O, are almost unobservable from Earth or spacecraft. The existing data on these species is limited to mere detection, with little or no information on time variability. Sodium, and the even rarer element potassium, are the only elements sufficiently visible to allow good time-resolved measurements. Although atomic sodium probably makes up only ~1 percent of the atmosphere and neutral clouds, its larger oscillator strength for resonant scattering far outweighs its scarcity. (See Brown and Yung, 1976, for a full discussion of the resonant scattering process.) Since its discovery 15 years ago sodium has been used as a tracer for the atmosphere and clouds of Io. Observations of potassium are scarce, but its behavior is similar in nature to the sodium cloud (Trafton, 1977). In the sections that follow, comments are therefore confined to the behavior of the sodium cloud. We then compare this behavior to the predictions, bearing in mind the caveats outlined in the first section of the chapter concerning the uncertainties about the sodium supply process.

Long-Term Behavior

The sodium cloud is a staple feature of the jovian system; it is always present at approximately the same brightness. To be more quantitative about this apparent constancy requires a comparison of data from a varied suite of instruments, techniques, and observers. Furthermore, the cloud exhibits a number of time variabilities caused by geometrical effects. Figure 34 shows the approximate shape of the cloud; as it orbits about Jupiter its projection on the sky obviously changes. Although such variations are clearly useful in deconvolving the shape of the cloud, they must be separated from true temporal variation in the density of the cloud. Furthermore, the Io-sun Doppler-shift also oscillates with an amplitude of ±17 km/s, varying the solar flux available for resonant scattering by an order of magnitude. Strictly speaking, one can therefore compare only observations obtained at identical orbital and magnetic longitudes. A large body of data and a good modeling capability are clearly required to remove these geometrical effects.

The quantity we use for comparison is the intensity of sodium emission within a radius of ~2.5 arcseconds of Io. This location was chosen as subject to the least dependence on observing geometry and the known short-term variabilities (although there remains a nonnegligible dependence on seeing conditions). Physically, 2.5 arcseconds corresponds to Io's $\sim 10^4$-km radius Hill sphere (sometimes called the Lagrange sphere), which encompasses the region where Io's gravity dominates. Observationally, this is slightly larger than the typical seeing disk. It is still necessary to compare emission intensities derived from different observational methods. This requires knowledge of how the emission is distributed in Io's vicinity. In reality, the brightest emission is not generated against Io's one-arcsec disk itself (where sodium is practically invisible due to a lack of contrast [Brown and Yung, 1976]) but from a ring surrounding Io. Under typical seeing conditions, however, the emission is so severely blurred that it covers Io's disk. The measured intensities therefore may be used for relative comparisons, but should not be directly inverted to column abundances without allowance for the effects of seeing.

Table 11 shows emission intensities derived by three methods. Most measurements were made with Io near elongation, but no attempt was made to correct for the dependence of intensity on Doppler shift. The emission intensity near Io can be directly measured by high-resolution spectroscopy (Brown et al., 1983; Schneider et al., 1987) with Io placed on the spectrograph entrance slit. The slit used by Bergstralh et al. (1977) was much larger, and the absolute intensity calibration was performed differently. For imaging studies (Morgan and Pilcher, 1988; Goldberg et al., 1984), where Io's disk must be occulted, the near-Io intensity must be derived from the intensities farther out. Given these limitations, we suspect the accuracy of the intensity calibration between observational methods is only good to the 50 percent level.

The primary result is that no very large variations or secular changes have taken place in the brightness of the Io sodium cloud over a twelve-year period. Given the uncertainties in the relative calibrations and the existence of short-term variations, the intensities in table 11 are consistent with a sodium cloud unchanged within a factor of two through the years. The scatter in the data from Bergstralh et al. (1977), obtained over a two-year period with the same instrumentation, rarely exceeds 50 percent. In addition, the basic shape of the cloud has apparently remained constant since its discovery. Although the actual shape was not successfully deconvolved until 1975 (Murcray and Goody, 1978; Matson et al., 1978), all previous and subsequent observations are consistent with that shape.

Little more can be said at present about the long-term constancy of sodium within Io's Hill sphere. Long-term variations due to plasma properties or volcanic activity are probably present, but the current data are not sensitive to intensity changes smaller than a factor of two. Such variations would be hidden in the broader variations due to imperfect intensity calibration, geometrical effects, changing Doppler shifts, variable seeing conditions, and short-term variations. Through the reduction of old observations and the careful acquisition of new data it will be possible to build a data set sufficient to detect long-term variations.

The constancy of the sodium cloud should be contrasted with the results for the visible sulfur ion emissions. Coverage is not as complete for ion measurements, but Trauger et al. (1980) and Trauger (1984b) present data which demonstrates that the S^+ density in Io's vicinity was lower by an order of magnitude in 1976

Table 11. Stability of the Io Sodium Cloud (≤3″ from Io)

Year	Date	Observation	Brightness (kR)	Reference
1974	July–Sept.	slit averaged	30–60	Bergstralh et al. (1975, 1977)
	Nov. 17	1-D profile	~30	Brown et al. (1975)
1975	Nov.–Dec.	slit averaged	30–60	Bergstralh et al. (1977)
1976–1979	(many)	slit averaged	?	Goldberg (1987)
1981	March–June	2-D images	~30	Goldberg et al. (1984)
1984	June	2-D images	~30	Morgan and Pilcher (1988)
1985	Aug.–Sept.	1-D profiles	20–40	Schneider et al. (1987)

than 1981–1983. Curiously, the sodium cloud somehow remained approximately constant (Murcray and Goody, 1978; Goldberg, 1987). Such a situation is clearly intriguing and important, but no explanation for such a juxtaposition has been proposed. We examine several possibilities in the section titled Feedback Loops between Neutrals and Ions.

Short-Term Behavior

On a time scale of hours, numerous periodic changes in the density, shape, and velocity distribution of the sodium cloud become apparent. These variations are primarily sensitive to the interactions between the plasma and the extended neutral clouds, but with care certain variabilities can be used as a probe of the atmosphere itself.

Magnetic Longitude Variations The importance of the plasma equator tilt was first revealed in observations by Trafton (1980, and references therein). They discovered an alternating asymmetry to the extended sodium cloud, with the brightnesses north and south of Io anticorrelated, highly variable, and oscillatory with a 13-hour period (fig. 40). This is precisely the result expected from the preceding discussion of ionization lifetime for sodium out of the orbital plane. From this variation, Trafton was able to determine the speed of the sodium and the electron temperature. Observations of this type provide a relatively simple means of measuring plasma conditions remotely.

Trafton and Macy (1977) also recorded high-resolution spectra of sodium within 10″ (20 Io radii) of Io. All spectra show a skirt to higher velocities, extending up to 18 km/s. Although the number of observations was small, they see a tendency for larger high-velocity populations when the plasma plane passed by Io. Brown and Schneider (1981) report a similar correlation in the appearance of very fast sodium (10–100 km/s) at a distance of 10 R_J from Jupiter. They detected high-speed sodium in only 2 of 17 combinations of Io magnetic and orbital longitudes. Both occurrences traced back to a recent passage of the plasma plane through the sodium cloud, with the cloud situated such that the fast sodium was directed into the field of view. These two types of variation would be expected based on the discussion of the first section of the chapter; collision and charge-exchange products are preferentially ejected when the plasma plane intersects the neutral clouds.

Systematic variations are also apparent in the overall shape of the sodium cloud. Pilcher et al. (1984) and Goldberg et al. (1984) have observed on many occasions the so-called "directional features," which appear north or south outside of Io's orbit. Figure 41 shows an

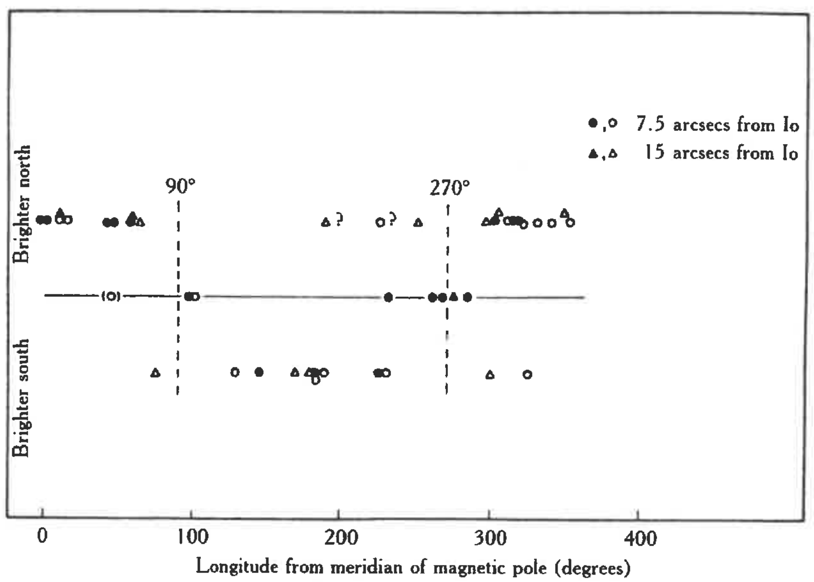

Figure 40. Magnetic longitude variability of the Io sodium cloud. The symbols show the sign of the difference in sodium D-line emission intensity for points symmetrically placed north and south of Io plotted against Io's differential magnetic longitude. In this system, 0° occurs when Jupiter's north magnetic pole is pointed toward Io. Data flagged with "?" may have been subject to an error in the sign of the offset. From Trafton (1980).

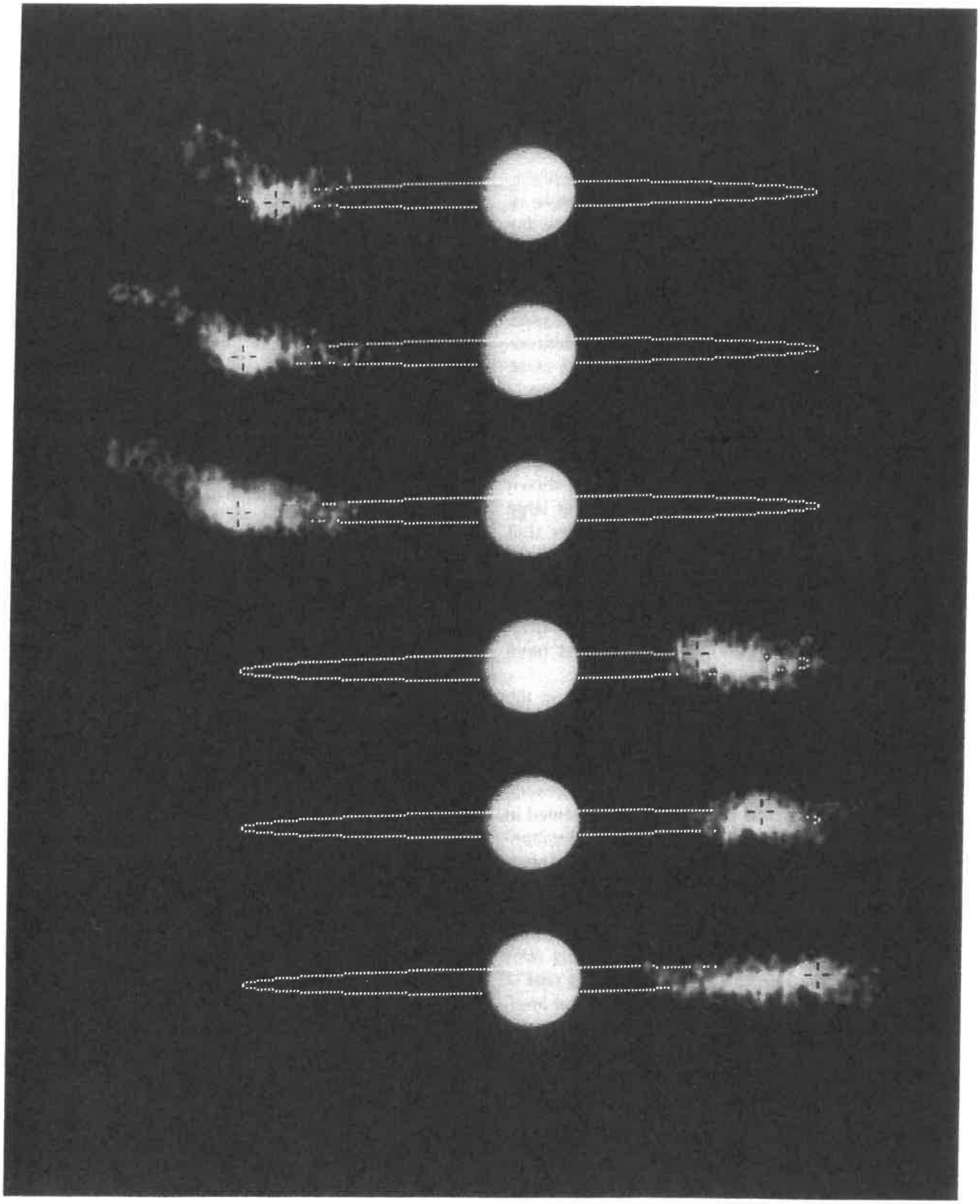

Figure 41. Images of Io's sodium cloud from Goldberg et al. (1984). The top frames show "directional features" extending to the north. A comparison of the third and sixth frames reveals the stretching of the cloud at western elongation due to radiation pressure.

example from Goldberg et al. These features are apparently caused by sodium ejected from Io primarily perpendicular to the orbital motion with velocities of 20 km/s. The north-south asymmetry is caused by preferential ionization at the plasma equator, which oscillates about Io's orbital plane. The Pilcher et al. analysis of the directional features is an excellent example of the power of time-variable phenomena in probing the torus-atmosphere interaction. Modeling of the north-south variation showed that a new population of energetic atoms was required, with a source rate comparable to the previous total source rate. Atomic physics calculations (Sieveka and Johnson, 1984) demonstrated that this could in fact be supplied by a close interaction between Io's atmosphere and the plasma.

Diurnal-Orbital Variations The most extensive published survey of sodium cloud intensities very near Io was performed by Bergstralh et al. (1977) and is shown in figure 42. These data revealed not only the large modulation caused by the effect of Io's Doppler shift through the solar Fraunhofer line, but also a small, yet measurable, tendency toward higher cloud intensities when Io was on the east side of Jupiter. This general trend also appears on a larger spatial scale in the imaging data of Goldberg (1987), but has not yet been quantified.

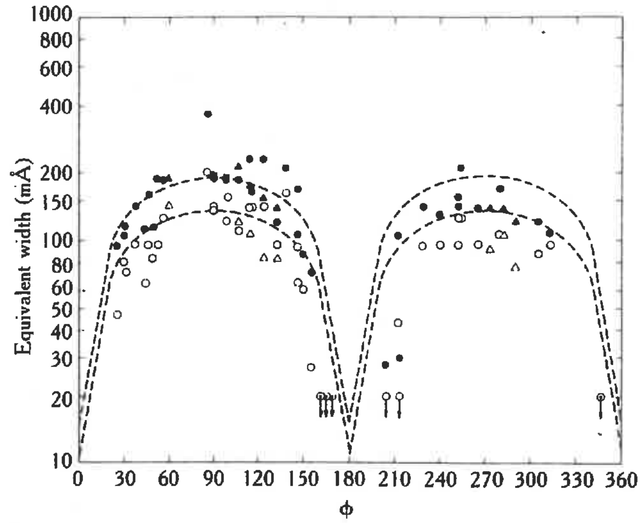

Figure 42. East-west intensity asymmetry of the sodium cloud from Bergstralh et al. (1977). Brightness of the sodium emission as a function of heliocentric orbital longitude. 0° longitude corresponds to superior heliocentric conjunction, with Io behind Jupiter. The *dashed lines* show the predicted variation due to Io's Doppler-shift motion through the deep solar fraunhofer line. *Open circles* show the D_1 line; *closed circles* show the stronger D_2 line. The slit measured 3″ by 8″ and was centered on Io's disk. Note that the emission east of Jupiter (0–180°) was slightly brighter than that west of the planet.

The east-west asymmetry is not surprising in the context of the processes described in the first section of the chapter, and two explanations have been proposed. Thomas (1986) suggests that the asymmetry is a diurnal effect caused by the large difference between the nightside and dayside atmosphere, as presented in figure 38. In this model, sodium atoms are underabundant in the thick atmosphere. Thus, the supply of sputtered sodium atoms is higher when the corotating plasma strikes the nightside surface (on the east of Jupiter) than when it strikes the dayside atmosphere (on the west). The difference in the sputtering rates results in a brighter sodium cloud when Io is east of Jupiter. Thomas's theory works at a mathematical level, but certain assumptions require confirmation. Although it is certainly plausible that the sodium content in the atmosphere is low (due to inhibited surface sputtering, for example), there is no direct evidence of such an effect. Recent experimental work by Chrisey et al. (1987) has shown that Thomas's calculations of the sodium supply rate from the surface are overly optimistic. It is also probable that the velocity distributions for ejection from the surface and atmosphere would be radically different. But given the uncertainty surrounding the nature of sodium atoms on Io's surface, and the possibility of a large day-night atmospheric asymmetry, a diurnal effect similar to Thomas's cannot be ruled out. Note that for this model, the supply of sulfur and oxygen would be enhanced when that of sodium is diminished.

Smyth and Combi (1987) have developed a model that incorporates the observed east-west asymmetries of the ionized species as well as neutral sodium. Both the Voyager ultraviolet spectrometer (UVS) experiment (Sandel, 1987) and ground-based observations (Morgan, 1985) indicate that the plasma at Io's orbit is hotter and denser on the west of Jupiter than on the east. This has been interpreted as evidence for an east-west electric field of ~3 mV/m, which effectively displaces the plasma inward or outward by $0.15R_J$ on opposite sides of Jupiter. Io is effectively moved to a denser region of the plasma when Io is west of Jupiter. Sodium is ionized more rapidly there, making the cloud fainter when Io is at western elongation. Smyth and Combi suggest that ground-based monitoring of the sodium cloud, especially at certain sensitive longitudes, may yield a direct measurement of the electric field strength, which may also be time-variable. In this model, only the sodium cloud exhibits a strong orbital asymmetry, since only its lifetime (see table 7) is short enough to generate an observable effect.

At a qualitative level, the sodium cloud morphology also varies as a function of orbital longitude. When Io is west of Jupiter, the cloud extends farther along the orbit than at eastern elongation (fig. 41). Smyth (1979, 1983) proposed radiation pressure as the cause, noting that through resonant scattering, the sodium atoms experience an acceleration away from the sun. The radiation pressure effectively stretches the cloud along Io's orbit when Io is west of Jupiter, and compresses it east of Jupiter. Detailed computer modeling can reproduce the general shape variations as long as the most probable velocity of the flux distribution of sodium atoms is ~2.6 km/s.

Recent very long exposures with the International Ultraviolet Explorer (IUE) satellite have yielded the first spectra of neutral oxygen and sulfur in Io's atmosphere and corona (Ballester et al., 1987, discussed further by Strobel, this volume). Although the data cannot be explained by the prevailing view of Io's interaction with the plasma, some rough interpretation is still possible. The four spectra obtained (two each at eastern and western elongation, viewing the downstream and upstream hemispheres, respectively) show no significant differences. The emission may be generated by electron impact excitation; this process should not differ greatly between the upstream and downstream hemispheres since the electron thermal velocities will greatly exceed the corotation velocity. The comparable emission rates therefore argue against a large upstream-downstream atmospheric asymmetry. If the emission region is large compared to Io, this is easily satisfied. Further interpretation of the spectra is required before firm conclusions may be reached.

Variations in Energetic Sodium Jets In addition to the above systematic behavior are some unexplained variations, most notably in the highest-speed sodium. The charge exchange reaction that produces such sodium is quite target-selective; even though sodium is a small percentage of both the atmosphere and torus, the reaction proceeds far more efficiently when a sodium ion collides with a sodium atom (McGrath, 1988). The fast neutral products, at average velocities of ~70 km/s in the Jupiter reference frame, can be observed by ground-based instruments with sufficient sensitivity and velocity resolution.

Trauger (1984b) has obtained velocity-resolved images of a high-speed jet emanating from Io's disk and extending forward along its orbit. These fast neutrals are probably the result of charge-exchange reactions taking place in Io's corona. Figure 43 shows an example of a high-speed jet; the jet is always present in Trauger's data and the vertical shape of the feature is basically a map of Io's extended atmosphere on a scale unobtainable through standard imaging techniques. On other occasions, Trauger (1987) has observed "tilted jets" not attached to Io but recently ejected from it. Both the tilt and the timing may be related to the tilted magnetosphere, but more analysis is required.

Schneider et al. (1987) have obtained high-resolution slit spectra of sodium at moderate distances from Io (~15", or 30 Io radii) and have documented the huge variability of the outer parts of the sodium cloud. Figure 44 shows several examples of high-speed sodium ejection from Io. In some extreme examples, the forward cloud is completely dominated by the rapidly escaping atoms. Note also that the jet typically appears north or south of the slow sodium. Both the directionality and the strength of these jets are highly variable in Schneider's data. This underscores the difficulty in interpretation of sodium cloud images without velocity information: The appearance of the outer parts of the sodium cloud during such bursts of charge-exchange products may have little to do with the behavior of the much slower "normal" cloud.

Several aspects of the high-speed sodium ejection events are unexplained but tantalizing. The jets observed by Trauger extend straight forward from Io and are only a few Io radii in cross section. Those observed by Schneider et al., however, typically extend out of the orbit plane, and are tens of Io radii in cross section. Despite their different morphologies, the velocity distribution of both phenomena indicate charge exchange as the source. Furthermore, there is currently no explanation for the north-south asymmetry of the Schneider observations. At the measured velocities of up to 70 km/s, sodium leaves the hot, dense torus before electron impact ionization can have any measurable effect. The north-south asymmetry may therefore arise from out-of-plane initial ejection velocities, for which there is no clear explanation. Further observations of this bizarre type of event will be required to uncover its significance.

Observed Behavior Versus Predicted Behavior

A host of periodic variations are well established in the extended sodium cloud. Most are adequately explained by the oscillating sink of the hot, dense plasma. These have been and will continue to be useful tools for remote sensing of the extended clouds and plasma.

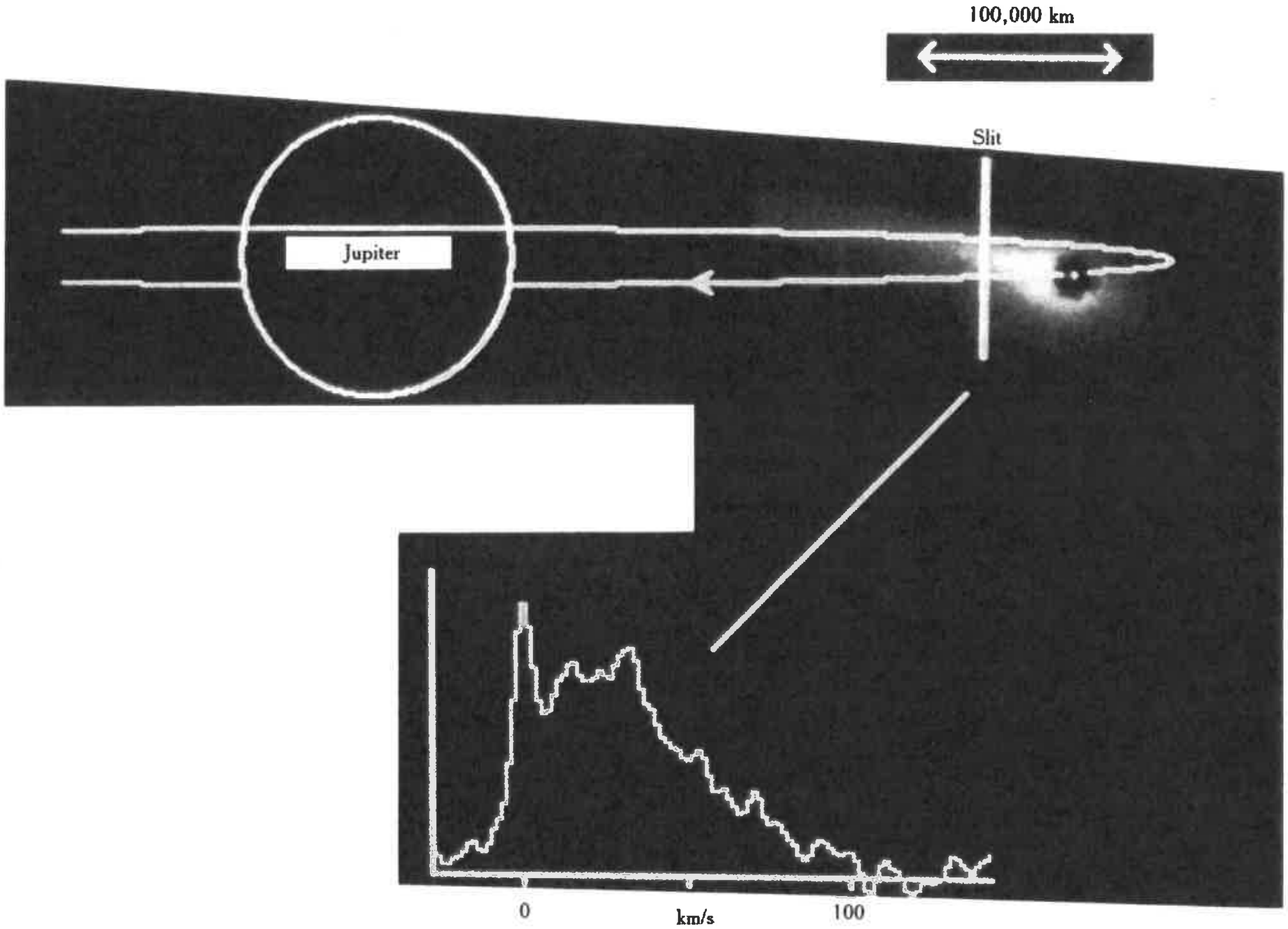

Figure 43. Simultaneous imaging and high-resolution spectroscopy of Io's sodium cloud on 17 June 1984 at 8:45 UT. Image taken by J. S. Morgan at the 2.2-m telescope on Mauna Kea. The white ellipse shows the projection of Io's orbit on the plane of the sky. Io itself is blocked by an occulting disk that is about four Io diameters across. Note that the bulk of the forward cloud does not lie along the projected orbit, but is well north of it. The simultaneous spectrum below by Schneider et al. (1984) obtained at the position of the line labeled "slit" reveals the velocity distribution. About 70 percent of the sodium emission in the region of the slit comes from atoms with velocities above 8 km/s with respect to Io. The spatial cross section of fast sodium feature is much larger than Io itself, unlike the jets observed by Trauger.

Other observed variations (or lack thereof) permit us to apply new constraints to the various atmospheric models. The long-term stability and the east-west orbital asymmetry are the most important results for uncovering the nature of the atmosphere.

The average sodium emission near Io has remained steady within a factor of two, based on two years of consistent monitoring by Bergstralh et al. (1977) and sporadic observations by a number of observers over the 15 years since Brown's discovery of the cloud. Although the relationship between supply to the sodium cloud and the cloud's intensity is under debate (see next section), we interpret the relative constancy of emission as indicative of a fairly steady supply of sodium from Io.

The sputtered corona model easily meets this requirement; it is, in fact, fairly difficult to change the supply rate by large factors. The sublimated atmo-

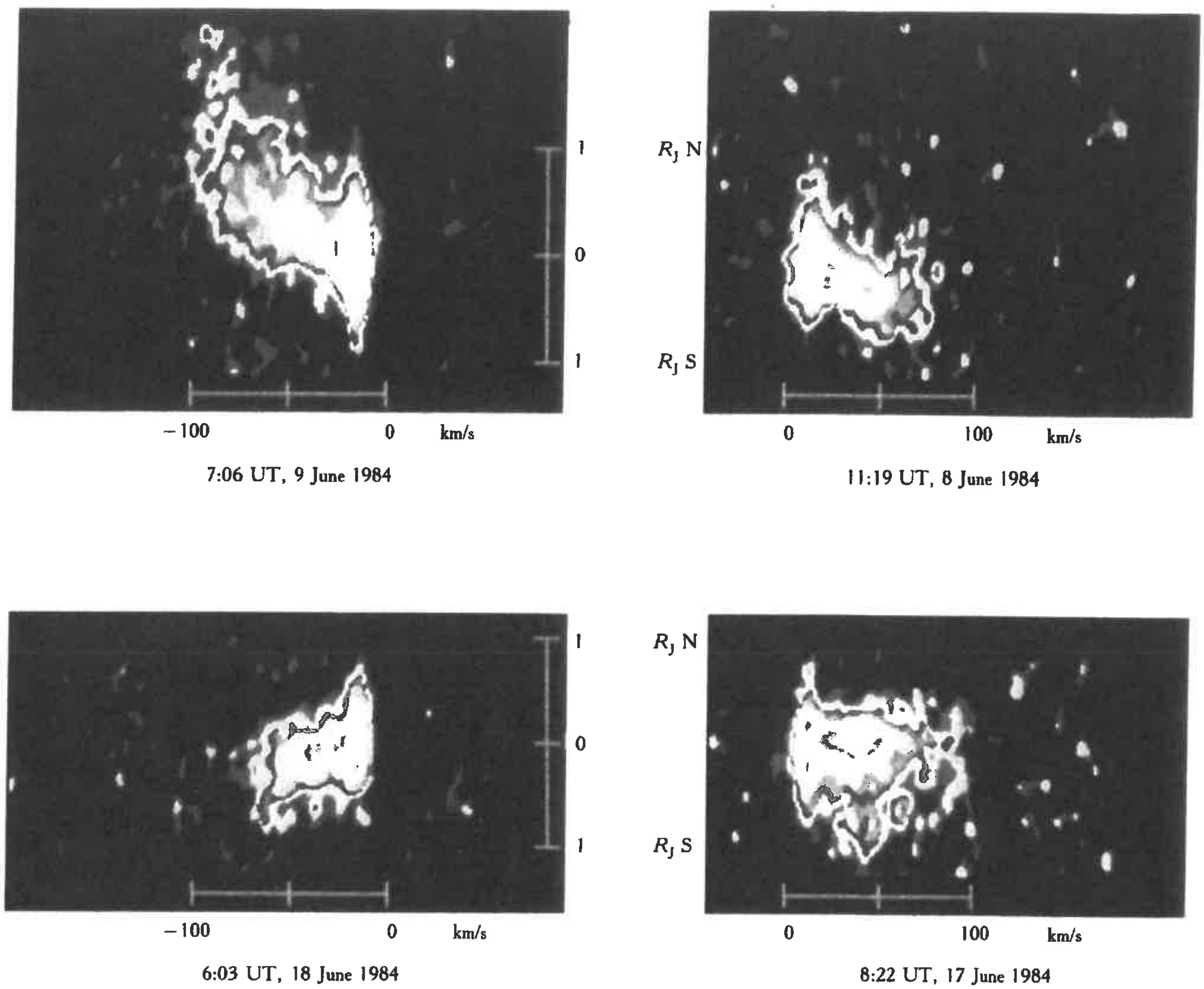

Figure 44. High-resolution spatially-resolved fast sodium spectra by LPL Echelle spectrograph and intensified CCD of the Io sodium cloud from Schneider (1988). The two left spectra were obtained when Io was east of Jupiter, and the two right spectra were taken with Io west of Jupiter. The slit was placed 0.67 R_J inside Io's position, oriented perpendicular to the orbital plane. Doppler shifts up to 100 km/s are present, and the fast sodium appears preferentially north or south of the slow sodium.

sphere model also predicts a fairly constant supply rate, as long as the exobase altitude does not vary with time. We can with some confidence rule out some extreme models, in which the exobase varies from 0 km to 900 km altitude; the supply rate would then vary by an unacceptably large factor of 3.4. The sulfur and oxygen supply from the volcanic atmosphere model proposed by Moreno et al. (1987) would change by a factor of ~4 to 20 with the appearance and disappearance of large plumes; we assume the sodium supply would strongly vary but cannot further quantify it. The available data cannot eliminate the volcanic atmosphere model, but it seem improbable that the sodium cloud would vary at most by a factor of two whereas the other species changed more drastically. We are again limited by our knowledge of the specific source of sodium.

The issue of the east-west orbital asymmetry of the neutral clouds is important in discriminating among atmospheric models, and merits further theoretical and observational work. The data indicate that some process causes a brighter sodium cloud east of Jupiter. Thomas (1986) invokes a time-variable sodium source (caused by a day-night atmospheric asymmetry) and a constant sink; Smyth and Combi (1987) use a constant sodium source but a variable sink (caused by the east-west electric field). Each is difficult to refute, and both effects may in fact be active. Based on the figures in table 8, large atmosphere-generated asymmetries are to be expected; the small observed effect may indicate the presence of a significant nightside atmosphere. Further effort must be applied to the sputtered and sublimated atmosphere models, and the cloud asymmetry that would arise from them. The process that liberates atomic sodium is central to this entire issue, and clearly demands further attention in cosmochemical theories and in laboratory experiments.

The symmetry of O and S emissions in the IUE spectra east and west of Jupiter clearly has a strong bearing on this issue, but the apparent inconsistencies of the emission excitation mechanism must be resolved before stronger conclusions can be reached. Ultraviolet observations such as these are difficult but important since they measure the dominant atmospheric constituents. If the atmospheric asymmetry effect dominates, coronal O and S densities should be higher west of Jupiter; the east-west electric field leads to no such asymmetry.

The high-speed jets near Io remain enigmatic. Their unexplained timing and north-south directionality lie outside our current understanding. The relationship between the directional features (which involve medium speed sodium directed at right angles to Io's orbit) and the very-high-speed jets (very fast sodium directed tangent to the orbit) also remains to be established. The sodium jets are more than isolated curiosities, since they imply the existence of similar jets of neutral oxygen and sulfur, greatly enhanced by the increased oxygen and sulfur densities in the atmosphere and plasma. The energy and mass that the oxygen and sulfur charge-exchange jets convey may be comparable to that of the less energetic loss processes (Smyth and Combi, 1986).

FEEDBACK LOOPS BETWEEN NEUTRALS AND IONS

The Problem

In the discussion so far, all the variabilities have been discussed as though the plasma responsible for sputtering, ionization, and the like was unaffected by its interactions with Io and the neutral clouds. The situation is, of course, quite to the contrary: The incident ions were themselves sputtered from Io and ionized only days or weeks before. The ions and neutrals are closely coupled by feedback loops conveying the mass and energy of the system.

In the presence of the variabilities measured and postulated above, one is compelled to ask what mechanism makes the feedback loops stable—what process returns the system to its equilibrium state. At the core of the complex reactions between ions and neutrals is the basic fact that the plasma torus generates itself: The corotating ions lift the neutrals off of Io, and the electrons ionize them. In this narrow view, we have an unstable positive feedback loop, where ions beget more ions, ad infinitum. Although such a scenario may have played a role in the startup of the neutral and ion tori, some mechanism currently limits the progression of mass and energy through the system. At present, there is no general agreement on the limiting process, and the current equilibrium point is not understood. In fact, there is no consensus on the expected effect of, for example, a short- or long-term doubling of the volcanic output.

The identification of this mechanism (or mechanisms) is extremely critical for the correct interpretation of the time-variability of the system. The same processes that keep the ion-neutral tori from blowing up or fading away act to restore the system to equilibrium after perturbations. The nature and time scale of the response to perturbation will be characteristic of the dominant rate-limiting process. Observations of time variations may help identify the process, and a proper mathematical analysis should provide further insights about the system not available through other means.

The purpose of the discussion that follows is not to answer the stability question, but to draw attention to our level of ignorance of this crucial issue. A number of ideas have been put forward, formally or informally, for rate-limiting processes. The following sections outline the basic precepts of each mechanism, derive rough predictions of the system response to supply rate changes, and discuss the shortcomings of the ideas.

Centrifugally Driven Diffusion

Huang and Siscoe (1986, 1987) have developed a mathematical formalism for dealing with simplified ion and neutral tori. They claim that the stabilizing mechanism is centrifugally driven diffusion, a nonlinear process in which the diffusion "constant" is actually proportional to the ion density. Figure 45a demonstrates the nature

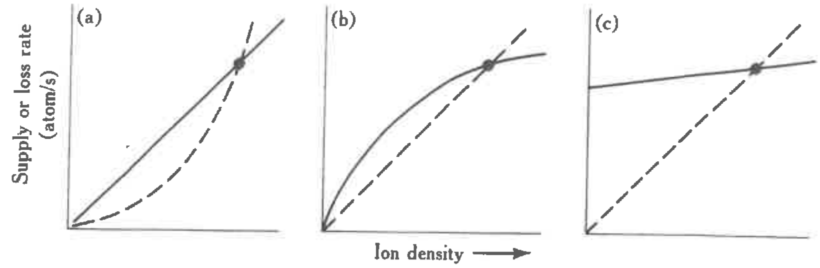

Figure 45. Three types of stability. The supply rate is shown as a *solid line*, and the loss rate by a *dotted line*. A stable equilibrium occurs at the intersection of the supply and loss curves if losses are increasing faster than the supply. (**a**) Nonlinear loss (centrifugally driven diffusion). The supply rate is proportional to the ion flux, and hence ion density. The loss rate varies as the square of the ion density, and always surpasses the supply rate at high densities. (**b**) Dynamic supply limitation (electron cooling, atmospheric buffering, and corotation breakdown). The supply rate is linear at low densities but tails off at higher densities. The linear loss rate is sufficient for system stability. (**c**) Atmospheric shielding. The supply rate is fairly constant with ion density. Linear loss rates can easily match the supply rate.

of the equilibrium. If the ion density increases, both the sputtering flux and the diffusive loss rate increase, but the latter increases faster. A stable equilibrium occurs at the intersection of the supply and loss curves.

The authors have used the equilibrium conditions to place constraints on the impedance of Jupiter's ionosphere and the effective sputter yield. These are difficult quantities to measure directly, which points out the usefulness of stability analysis in probing the torus system.

Huang and Siscoe also predict the response to perturbations in the ion and neutral densities. A transient rise in the neutral supply rate, according to this model, will increase the neutral density, which in turn leads to a marginal increase in the ion density. The excess ions would be dissipated by diffusion with a 60-day time constant, but the neutral excess disappears in about one day. The same calculations indicate that an ion perturbation would not in fact lead to a neutral density perturbation; this counter-intuitive result no doubt stems from the simplifications of the model, and therefore merits reexamination. They further calculate that a secular increase in the neutral supply rate would increase the neutral and ion densities. The unusual state of the torus in 1976 (as described in chapter 2) could not have been long-lived, but might have been due to a transient ion event as described above. The authors maintain that the level of volcanic activity should not affect the density of the ion or neutral tori, but this follows implicitly from their assumption of a strictly constant atmosphere. Eviatar (1987) makes the obvious point that the extent of the atmosphere may respond to the rate of volcanic outgassing. His quantitative estimates of this effect, however, are based on questionable assumptions regarding the importance of atmospheric condensation and the atmospheric area subjected to sputtering.

The key feature of this type of stability is centrifugally driven diffusion. Richardson and McNutt (1987) have recently presented evidence that this mechanism is not important in the Io plasma torus. They maintain that the characteristic signature of this type of flux-tube interchange is missing from the Voyager plasma science experiment data. If only linear diffusion occurs in the Io torus, some other mechanisms must stabilize the system. The other major criticisms of this model stem from the fact that the authors ignore the variability of certain parameters (e.g., the electron temperature and exobase location). The following models have been developed to address these issues.

Supply-Limiting Mechanisms

Stability can also be provided if the supply rate falls below the linear relation used above. In the following three subsections, different means of limiting the supply rate are discussed. In each of them, a linear loss rate (e.g., due to externally driven diffusion) is sufficient for stability.

Electron Cooling Huang and Siscoe assume in their stability model that the plasma temperature (and hence the rate constant for electron impact ionization) is independent of ion and neutral densities. But the Voyager plasma science (PLS) experiment (Sittler and Strobel, 1987) suggests that electrons near Io were significantly cooled, presumably by interaction with Io's dense neutral corona. Two effects lead to the cooling: (1) the energy loss of the incident electron in the process of electron impact ionization, and (2) the addition (from the ionization) of a new electron with negligible gyro-energy. The result is a cooler electron population near Io, less capable of ionizing neutrals than the original population. The electrons may also be cooled through radiative processes, which are very efficient at high densities.

Stability is achieved in this scenario (proposed by Shemansky, 1987) by reducing the ability of the plasma to add fresh ions. In effect, this mechanism stabilizes the supply rate instead of the ion or neutral densities. An increase in the neutral supply rate temporarily boosts the neutral and ion densities, but cools the electrons through ionization and radiative losses so that further ionizations are reduced. Thus the supply rate falls below the linear rate at some value (as shown in figure 45b). Ions are then lost through linear diffusion or other loss processes until the ion density returns to normal. In the meantime, charge exchange and elastic collisions have removed neutrals from the system, and have supplied sufficient energy to the ions to reheat the electrons.

This model is not fully developed, so only qualitative predictions are possible. For both short- and long-term increases in the supply rate the neutral clouds should be denser, and the electron temperature lower. The ion density remains fairly constant. Collisions and charge exchange will become increasingly important, so high-speed jets and directional features should become more pronounced. Without a full mathematical description it is difficult to appraise this stability mechanism critically. This mechanism does offer a solution to the torus "energy crisis" described by Shemansky (1988). He maintains that an additional source of energy (such as charge exchange, enhanced in this scenario) is required to power the torus; it remains to be seen if the amount of energy supplied is sufficient.

Atmospheric Buffering In this scenario, Io's exobase level strikes a balance between the supply from the surface (or volcanoes) and the losses from the top of the atmosphere. Increased volcanic activity, for example, may raise the exobase level, but a higher plasma flux will lower it. Johnson and McGrath (1987) have suggested this mechanism informally, but no calculations have been performed. As discussed in the section titled Overview of the System, the supply rate to the neutral clouds (and torus) depends linearly on the sputtering flux and on the cube of the exobase radius. The supply rate, then, is very sensitive to the exobase level.

Stability is again achieved by controlling the supply rate. At first, a rise in the neutral supply rate increases the neutral and ion densities. But the increased sputtering flux would erode the atmosphere, lowering the exobase and decreasing the supply rate. Note that the exobase must lie above the surface for this mechanism to function. If the exobase lies near the surface, a different mechanism is required. R. E. Johnson (1988) has suggested that a partially thick atmosphere might modulate the incident flux to the surface, and thereby limit both the atmospheric content and the supply rate.

This stability mechanism is difficult to criticize because it has no quantitative basis; the arguments are sound but the magnitude of the effects may not be sufficient to provide stability. Considerable work is required before it can be judged in a satisfactory way.

Corotation Breakdown The supply of ions to the torus (also called the mass-loading rate) causes the Io torus to lag behind corotation slightly, and this lower velocity in turn reduces the mass-loading rate. The observed corotation lag of several percent is due to the finite ability of the jovian magnetosphere to accelerate freshly created ions. A very large mass-loading rate reduces the speed at which ions impact Io; this lowers the sputtering flux, the sputtering yield per incident ion, and the energy input per ionization (or charge exchange). All of these effects serve to lower the ion supply rate and return the system to equilibrium.

Again, detailed predictions are not possible since the mechanism has only been qualitatively examined. The primary response to both temporary and long-term increases in the mass-loading rate is a decrease in the speed of the plasma. The plasma temperature will also be lower, but without further calculations it is impossible to determine how the ion and neutral densities will change. Obviously this mechanism must be studied more fully before its importance to the stability problem can be addressed. Preliminary calculations by Huang and Siscoe (1987b) suggest that the current value for the mass-loading rate is several orders of magnitude below the threshold for this effect. These calculations use many of the simplifications of the centrifugally driven diffusion model, so further examination of the corotation breakdown mechanism is required.

Atmospheric Shielding

The corotating plasma might not impinge directly on the Io atmosphere. The plasma will be deflected (fig. 46) if there are intrinsic magnetic fields, a conducting ionosphere, or electric fields induced by ionization or

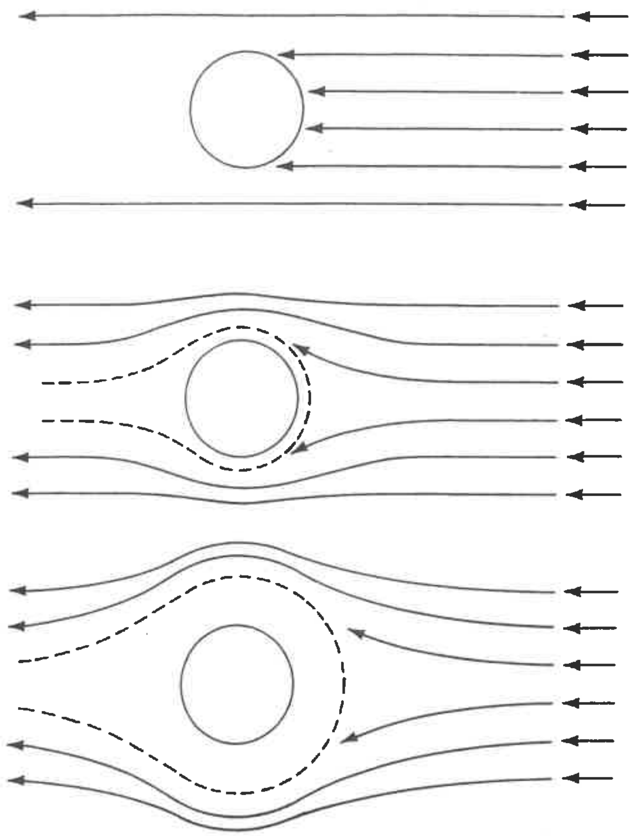

Figure 46. Plasma flow field for various amounts of flow deflection. The plasma can be diverted by an intrinsic magnetic field, a conducting ionosphere, or local electric fields.

charge exchange. Evidence for a deflection of this nature was obtained by the Voyager plasma science experiment (Barnett, 1986). If the flow is held off of Io's atmosphere, the supply to the torus will be determined by the upward flux of atoms and molecules from below the shielded region. For example, thermal escape may control the population of neutrals exposed to the plasma. Thus, as shown in figure 45c, the supply rate will be only weakly dependent on (or conceivably independent of) of the incident corotating flux. The stability problem vanishes: The neutral clouds and torus are driven by escape rates from Io that do not depend on conditions in the torus. Transient ion or neutral events should clearly have little effect on the system. Secular changes, such as an increase in volcanic activity, could affect the level of plasma deflection and/or the escape rate, thereby leading to variations in the supply to and densities of the neutral clouds and torus. The level of change will depend on the physics of the plasma deflection, which is uncertain at present. This scenario cannot be critically appraised without a better understanding of the interaction of the plasma flow and the atmosphere and/or surface. It is appealing, however, since it cleanly explains the stability of the torus system, and the lack of large variations in the sodium cloud.

Stability Summary

It is remarkable that no consensus has emerged on an issue as fundamental as the stability mechanism for the torus, and the diversity of competing idea suggests that no agreement is forthcoming. The correct explanation may not even be on the current list. Each model discussed here requires a considerably more realistic and rigorous treatment, synthesizing the state of knowledge of surface, atmospheric, and magnetospheric physics, and in particular the interaction of the plasma with Io's atmosphere. Each model must be developed sufficiently to make predictions about the individual components (especially the observable components) of the system: the dense atmosphere (if any), the neutral corona, the extended neutral clouds, and the plasma torus. Until this analysis is complete, it is difficult to directly compare predictions of the different models.

One contributing cause to the slow development of stability models is the general lack of data that adequately describe a departure from equilibrium. Observations must capture the full context of the state of the system, at minimum near simultaneous measurements of the neutral and ion densities. A few examples of this essential type of observational coverage do exist. In 1976, for example, the data of Murcray and Goody (1978) and Goldberg (1987) indicate the shape and intensity of the sodium cloud are consistent with the long-term average state of the cloud. Yet Trauger (1984a) reports a substantial difference in the torus density near Io between 1976 and subsequent times. The ion torus was apparently quite different in density and/or temperature; the proposed models of the feedback mechanism are insufficiently developed to compare with this unusual situation in 1976.

CONCLUSIONS AND DISCUSSION

All of the important processes affecting the Io atmosphere and neutral clouds are strongly time-variable, with time constants ranging from hours to years. The study of neutrals near Io has profited dramatically from observations of the changing state of the sodium cloud, allowing remote sensing of the clouds and plasma that would not have been possible in a more constant system. Opportunities abound for further applications of the use of time-variable phenomena in exploring the Io torus system. The conclusions reached below are constrained by two fundamental limitations: (1) we do not know to what extent the plasma is altered or diverted by Io and its atmosphere and (2) we do not know how the process that releases sodium from the surface is related to the process that releases SO_2.

Three widely different atmospheric models have been suggested, and each has its own characteristic variations. Even though the subsolar surface density differs by four orders of magnitude between models, the difference in supply rate to the neutral clouds among models is closer to one order of magnitude, and the time variations within a model may be even smaller. Such differences are at the limit of detectability. The variabilities for the most part have different characteristic time scales: The sputtered corona should show systematic variabilities with periods of 6.5, 13, and 42 hours; the sublimated atmosphere should be driven primarily at 42 hours; and the volcano-generated atmosphere should vary sporadically on a time scale of days to months.

The strongest observational result is the fairly constant level of sodium emission over periods of days to years. This single fact must be accounted for in any atmospheric model and allows limits to be placed on the variations in proposed atmospheres. Large changes in the surface density of Io's atmosphere (determining whether the atmosphere is collisionally thick, and where the exobase is) lead to an unacceptably large sodium cloud variation; if volcanoes are currently driving the exobase level, then the eruption rate has probably endured for at least the 15 years since the discovery of the sodium cloud. Strong variations on the time scales of days to weeks are not observed: Either the exobase level is not strongly dependent on individual volcanic eruptions, or the sodium supply is somehow independent of these eruptions.

Perhaps the most valuable contribution variability analysis can provide is information on the diurnal structure of the Io atmosphere. Since it is virtually impossible to directly measure Io's nightside atmosphere from the Earth, the variability of the neutral clouds may be our best clue. The observed east-west intensity asymmetry of the sodium cloud has been alternately interpreted as evidence for an asymmetric, sublimated atmosphere, or a more uniform global atmosphere affected by an electric field across the magnetosphere. Only combined advances in theory, observation, and laboratory measurement will resolve this question.

The stability of the feedback loops in the torus has effectively been taken for granted over the years. This luxury can no longer be afforded, now that our understanding of the individual components of the system has revealed their complex interdependence. Our review of stability mechanisms is not intended to answer the problem, but rather to highlight it. None of the five scenarios presented can be accepted as it stands, but each demonstrates an important link of the interconnections of the atmosphere, neutral clouds, and plasma torus.

The debate over the nature of the Io atmosphere and the torus-stabilizing mechanism will remain heated for years to come. Observations that attempt direct measurements of important quantities (e.g., the atmospheric column abundance) are clearly needed, but further studies of the time-variable phenomena are a powerful indirect means of answering many of the same questions. Each atmospheric model and each stability mechanism has its own characteristic response to long- and short-term perturbations and may be identified through them.

UNRESOLVED PROBLEMS AND FUTURE WORK

The rich variety and incisive nature of variable phenomena in the atmosphere and neutral clouds warrant a healthy and deliberate monitoring, data reduction, and analysis program. This must be supported by corresponding advances in theory and laboratory work.

Observations

In recent years, observations of the sodium cloud have used advanced instrumentation to address small, well-defined problems. Instrumentation has improved dramatically since the systematic observing programs of the 1970s; application of the same effort with current equipment would provide a vastly more powerful data set. Further measurements of the east-west intensity asymmetry in the cloud are required, with sufficient coverage to determine the effect of magnetic longitude at all orbital longitudes. A concerted effort should be applied to a determination of the orbital longitudes of maximum and minimum sodium brightness; in both proposed asymmetry explanations, supply or loss is maximized at orbital elongation, so the phase lag of the density modulation may be revealing. Systematic coverage will also provide the best measurements of any long-term variability, especially if it is obtained with a fixed instrument configuration.

The mutual eclipses of 1991–1992 provide another opportunity to study the near-Io atmosphere at subarcsec resolution. The radial profile of sodium in the corona is straightforward to measure (Schneider et al., 1987); if enough eclipses are observed, orbital and magnetic longitude effects should be measurable.

Ultraviolet observations provide our best clue about S and O in the vicinity of Io. Observations with IUE (Ballester et al., 1987) should continue, with particular attention to quantifying and explaining any differences between the upstream and downstream hemispheres. The implied possibility of bright visible O auroras (5577 Å, 6300 Å) on Io should be explored. The UV capabilities of the Hubble Space Telescope will be even better suited to address a number of fundamental issues concerning Io's atmosphere. The improved instrumentation and high spatial resolution will permit an accurate mapping of the O and S emissions in Io's vicinity, and their orbital asymmetries. Unambiguous measurements of SO_2 in the atmosphere may be possible. Other Earth-orbital facilities may complement Space Telescope's capabilities.

When feasible, observations of neutral species should be carried out in conjunction with observations of the ionized species; the plasma context is required for correct interpretation of neutral measurements. It has recently become possible (Smyth and Combi, 1988b) to combine the model results from the few existing data sets containing both ion and neutral measurements. This type of data is extremely powerful for deciphering the interaction of the plasma torus and the neutral clouds.

It is critical not to overlook the wealth of existing observations that lies unreduced and unpublished. The power and convenience of modern image processing systems make the task of reduction much more manageable than when the data were taken. The hundreds of unreduced images and spectra are important not only in their own right but also in completing the timeline of sodium cloud behavior over the past decade.

Theoretical Work

We urge a more thorough and uniform development of theoretical models of the atmosphere and of the stability mechanisms to the point of detailed predictions for the atmosphere, corona, neutral clouds, and plasma torus. Our ability to measure changes in the volcanic activity is constantly improving (see Howell and Sinton, this volume), as are our capabilities for detecting small changes in the neutral clouds and plasma torus. How will the system respond to a doubling of the volcanic eruption rate? The lack of a unified theory to explain the combined variations must be addressed. The most difficult link in such a theory is interaction of the corotating plasma with Io's atmosphere. Does the plasma impinge directly on Io's surface or exobase? What causes the flow to stand off of Io, and how might it respond to variable volcanism? What determines the supply rate from Io?

Sodium's easy visibility has been a blessing and a curse, allowing easy measurements of a very minor constituent. Sodium observations tell us little of the atmosphere as a whole if it is released from the surface by totally different means than sulfur and oxygen. What forms may sodium take on Io's surface, and what are the implications for the sputtering process? What is the relative abundance of sodium compounds in the surface and atmosphere? Why have sodium and potassium survived generations of recycling of Io's surface? Does sodium play a role in the thermodynamics of the volcanic eruptions?

Laboratory Work

We have only begun to understand Io's surface and the role it plays in feeding the atmosphere and torus. Further sputtering experiments are called for, employing substances more closely resembling those expected on Io. Sodium-bearing compounds such as Na_2S and NaS_x are of particular interest. Hapke (1986) has recently suggested a mixture of polysulfur oxides, basalt, S_2O, and SO_2, and the sputtering properties of these should be determined. Surface roughness and porosity may also affect the sputtering process, and recent experiments (Nash, 1987; Nash and Moses, 1987) suggest that sulfur deposits may be very filamentary.

Our ability to measure UV emissions from Io has exceeded our ability to interpret them. Laboratory estimates of cross sections for electron-impact excitation, particularly on SO_2 and its byproducts, would greatly aid the interpretation of UV spectra. The advent of the greater resolution and sensitivity of the Hubble Space Telescope will certainly amplify this problem.

References

Ballester, G. E. (1987). Personal communication.

Ballester, G. E., H. W. Moos, P. D. Feldman, D. F. Strobel, M. E. Summers, J.-L. Bertaux, T. E. Skinner, M. C. Festou, and J. H. Lieske (1987). Detection of neutral oxygen and sulfur emissions near Io using IUE. *Astrophys. J.* 319:L33–38.

Barbosa, D. D., and M. G. Kivelson (1983). Dawn-dusk electric field asymmetry of the Io plasma torus. *Geophys. Res. Lett.* 10:210–213.

Barnett, A. S. (1986). In situ measurements of the plasma bulk velocity near the Io flux tube. *J. Geophys. Res.* 91:3011–3019.

Baumgardner, J., M. A. Moreno, G. Schubert, and M. G. Kivelson (1987). Two classes of volcanic eruptions and their corresponding atmospheres on Io. *Bull Am. Astr. Assoc.* 19(3): 856.

Bergstralh, J. T., J. W. Young, D. L. Matson, and T. V. Johnson (1977). Sodium d-line emission from Io: A second year of synoptic observations from Table Mountain Observatory. *Astrophys. J.* 211:L51–55.

Brown, R. A., and N. M. Schneider (1981). Sodium remote from Io. *Icarus* 48:519–535.

Brown, R. A., and Y. L. Yung (1976). Atmosphere and emissions of Io. In *Jupiter* (T. Gehrels, ed.), pp. 197–225. Univ. of Arizona Press.

Brown, R. A., C. B. Pilcher, and D. F. Strobel (1983). Spectrophotometric studies of the Io torus. In *Physics of the jovian magnetosphere* (A. J. Dessler, ed.), pp. 197–225. Cambridge Univ. Press.

Chrisey, D. B., R. E. Johnson, J. W. Boring, and J. A. Phipps (1987). Ejection of sodium from sodium sulfide on the surface of Io. Submitted to *Icarus*.

Eviatar, A. (1987). Volcanic control of the Io atmosphere and neutral plasma torus. *J. Geophys. Res.* 92:8800–8804.

Fanale, F. P., W. B. Banerdt, L. S. Elson, T. V. Johnson, and R. W. Zurek (1982). Io's surface: Its phase composition and influence on Io's atmosphere and Jupiter's magnetosphere. In *The Satellites of Jupiter* (D. Morrison, ed.), pp. 756–781. Univ. of Arizona Press.

Goertz, C. K. and W.-H. Ip (1984). A dawn-to-dusk electric field in the jovian magnetosphere. *Icarus* 32:179–185.

Goldberg, B. A. (1987). Private communication.

Goldberg, B. A., G. W. Garneau, and S. K. LaVoie (1984). Io's sodium cloud. *Science* 226:512–516.

Hapke, B. A. (1986). The surface of Io: A new model. *Bull. Am. Assoc.* 18(3): 774.

Huang, T. S., and G. L. Siscoe (1986). Stability of the Io torus. *J. Geophys. Res.* 91:10163–10166.

Huang, T. S., and G. L. Siscoe (1987a). Types of planetary tori. *Icarus* 70:379–382.

Huang, T. S., and G. L. Siscoe (1987b). Corotation lag limit on mass-loss rate from Io. *Astrophys. J.* 319:1003–1009.

Ip, W.-H., and C. K. Goertz (1983). An interpretation of the dawn-dusk asymmetry of UV emission from the Io plasma torus. *Nature* 302:232.

Johnson, R. E. (1988). Book in preparation.

Johnson, R. E., and M. A. McGrath (1987). Personal communication.

Johnson, T. V., and D. L. Matson (1989). Io's tenuous atmosphere. In *Atmospheres* (S. Atreya, ed.). Univ. of Arizona Press, in preparation.

Kliore, A., G. Fjeldbo, B. Siedel, D. Sweetman, T. Sesplaukis, and P. Woiceshyn (1975). Atmophere of Io from Pioneer 10 radio occultation measurements. *Icarus* 24:407–410.

Kumar, S. (1985). The SO_2 atmosphere and ionosphere of Io: Ion chemistry, atmospheric escape, and models corresponding to the pioneer 10 radio occultation measurements. *Icarus* 61:101–123.

Kumar, S., and D. M. Hunten (1982). Atmospheres. In *Satellites of Jupiter* (D. Morrison, ed.), Tucson. Univ. of Arizona Press.

Lanzerotti, L. J., W. L. Brown, W. M. Augustyniak, R. E. Johnson, and T. P. Armstrong (1982). Laboratory studies of charged particle erosion of SO_2 ice and applications to the frosts of Io. *Astophys. J.* 259:920.

Linker, J. A., M. G. Kivelson, M. A. Moreno, and R. J. Walker (1985). Explanation of the inward displacement of Io's hot plasma torus and consequences for sputtering sources. *Nature* 315:373–378.

Matson, D. L., B. A. Goldberg, T. V. Johnson, and R. W. Carlson (1978). Images of Io's sodium cloud. *Science* 199:531–533.

Matson, D. L., and D. Nash (1983). Io's atmosphere: Pressure control by regolith coldtrapping and surface venting. *J. Geophys. Res.* 88:4771–4783.

McEwen, A. S., and L. A. Soderblom (1983). Two classes of volcanic eruptions on Io. *Icarus* 55:191–217.

McEwen, A. S., L. A. Soderblom, T. V. Johnson, and D. L. Matson (1987). The global distribution, abundance and stability of SO_2 on Io. In preparation.

McGrath, M. A. (1988). Ph.D. dissertation, Univ. of Virginia.

McGrath, M. A., and R. E. Johnson (1987). Magnetosphere plasma sputtering of Io's atmosphere. *Icarus* 69:519–531.

Moreno, M. A., G. Schubert, J. Baumgardner, and M. G. Kivelson (1987). Volcanic eruptions and the atmosphere of Io. In preparation.

Morgan, J. S. (1985). Temporal and spatial variations in the Io torus. *Icarus* 62:389–414.

Morgan, J. S., and C. B. Pilcher (1988). Personal communication.

Murcray, F. J., and R. M. Goody (1978). Pictures of the Io sodium cloud. *Astrophys. J.* 226:327–335.

Nash, D. B. (1987). Sulfur in vacuum: Sublimation effects on frozen melts, and applications to Io's surface and torus. *Icarus* 72:1–34.

Nash, D. B., M. H. Carr, J. Gradie, D. M. Hunten, and C. F. Yoder (1986). Io. In *Satellites* (J. A. Burns, ed.), pp. 629–688. Univ. of Arizona Press, Tuscon.

Nash, D. B., and J. I. Moses (1987). More lab results on vacuum weathering of frozen sulfur: Applications to Io. *Bull. Am. Assoc.* 19(3): 855.

Pearl, J., R. Hanel, V. Kunde, W. Maguire, K. Fox, S, Gupta, C. Ponnamperuma, and F. Raulin (1979). Identification of gaseous SO_2 and new upper limits for other gases on Io. *Nature* 280:757–758

Pilcher, C. B., W. H. Smyth, M. R. Combi, and J. H. Fertel (1984). Io's sodium directional features: Evidence for a magnetosphere-wind-driven gas escape mechanism. *Astrophys. J.* 187:427–444.

Richardson, J. D., and R. L. McNutt (1987). Observational constraints on interchange models at Jupiter. *Geophys. Res. Lett.* 14:64–67.

Sandel, B. R. (1985). Displacement of the center of the plasma torus from Jupiter's magnetic dipole. *Bull. Am. Assoc.* 17:695.

Schneider, N. M. (1987). Velocity structure of the Io sodium cloud. *Bull. Am. Assoc.* 19(3): 854–855.

Schneider, N. M. (1988). Sodium in Io's extended atmosphere. Ph.D. dissertation, Univ. of Arizona.

Schneider, N. M., D. M. Hunten, W. K. Wells, and L. M. Trafton (1987). Eclipse measurements of Io's sodium atmosphere. *Science* 238:55–58.

Shemansky, D. E. (1987). Personal communication.

Shemansky, D. E. (1988). Energy branching in the Io plasma torus; the failure of neutral cloud theory. *J. Geophys. Res.* 93:1773–1784.

Sieveka, E. M., and R. E. Johnson (1984). Ejection of atoms and molecules from Io by plasma-ion impact. *Astrophys. J.* 287:418–426.

Sieveka, E., and R. E. Johnson (1985). Non-isotropic coronal atmosphere on Io. *J. Geophys. Res.* 90:5327–5331.

Sieveka, E., and R. E. Johnson (1986). Correction to "Non-isotropic coronal atmosphere on Io." *J. Geophys. Res.* 91:4608.

Sittler, E. C., and D. F. Strobel (1987). Io plasma torus electrons: Voyager 1. *J. Geophys. Res.* 92:5741–5762.

Smyth, W. H., and M. R. Combi (1986). Understanding the escape of material from Io and its role in the planetary magnetosphere. Paper presented at the Second Neil Brice Memorial Symposium, "Magnetospheres of the Outer Planets," September 1–5, 1986, Iowa City, Iowa. *Bull. Am. Assoc.* 16:663–664.

Smyth, W. H., and M. R. Combi (1987). Correlating east-west asymmetries in the jovian magnetosphere and the Io sodium cloud. *Geophys. Res. Lett.* 14(9): 973–976.

Smyth, W. H. and M. R. Combi (1988a). A general model for Io's neutral gas clouds. II. Application to the sodium cloud. *Astrophys. J.* 328:888–981.

Smyth, W. H., and M. R. Combi (1988b). Personal communication.

Smyth, W. H., and M. B. McElroy (1978). Io sodium cloud: Comparisons of models and two dimensional images. *Astrophys. J.* 226:336–346.

Thomas, N. (1986). An explanation of the east-west asymmetry of Io's sodium cloud. *Nature* 322:343–345.

Trafton, L. (1977). Periodic variations in Io's sodium and potassium clouds. *Astrophys. J.* 215:960–970.

Trafton, L. (1980). An explanation for the alternating north-south asymmetry of Io's sodium cloud. *Icarus* 44:318–325.

Trafton, L., and W. Macy (1977). Io's sodium emission profiles: Variations due to Io's phase and magnetic longitude. *Astrophys. J.* 215:971-976.

Trauger, J. T. (1984a). The jovian nebula: A post-Voyager perspective. *Science* 226:337–341.

Trauger, J. T. (1984b). Photometric images of sulfur ions and sodium neutrals in the Jupiter/Io torus. *Bull. Am. Assoc.* 16:712.

Trauger, J. T. (1987). Private communication.

Trauger, J. T., G. Münch, and F. L. Roesler (1980). A study of the jovian [S II] nebula at high spectral resolution. *Astrophys. J.* 236:1035–1042.

Watson, C. C. (1981). The sputter-generation of planetary coronae: Galilean satellites of Jupiter. *Proc. Lun. Planet. Sci. Conf.* 12:1569–1583.

Wolf-Gladrow, D. A., F. M. Neubauer, and M. Lussen (1987). Io's interaction with the plasma torus: A self-consistent model. *J. Geophys. Res.* 92:9949–9961.